REPORT NO. 131

May, 1960.

THE COLLEGE OF AERONAUTICS

CRANFIELD

An Experimental Study of the Lift and Drag of Single Wedge Sections in Two Dimensional Transonic Flow using the Hydraulic Analogy*

- by -

J. W. Bugler, B.Sc., D.I.C., D.C.Ae.

and

N. C. Hanslip, M.Sc., D.C.Ae.

SUMMARY

The similarity of the differential equations of the transonic flow of a gas in two dimensions and of the flow of shallow water led to the choice of the latter as an experimental method to determine the pressure distribution, lift and drag on wedges with total angles of 10°, 15° and 20°. The wedges were towed through shallow water and the wave pattern was determined by the measurement of water depth using a photographic technique. The results have been compared with theory and with wind tunnel experiments. For the 10° and 15° wedges the trends for a range of angles of incidence agree with the predictions from transonic small disturbance theory, whereas those for the largest wedge of 10° semi-angle indicate that this angle is too large to expect satisfactory experimental results. The trends are also similar to those obtained by other workers in a wind tunnel.

---

* Based on an experimental thesis submitted in partial fulfilment of the requirements for the Diploma of The College of Aeronautics. The thesis was edited and the final report prepared by Mr. J.L.Naylor.

CONTENTS

LIST OF SYMBOLS

a	Speed of sound
c	Wedge chord length
C_{Do}	Pressure drag coefficient
C_L	Lift coefficient
C_P	Pressure coefficient $= (p_L - p_U)/\frac{1}{2}\rho_\infty V_\infty^2$
ΔC_P	Increase in pressure coefficient due to incidence
C_{Po}	Stagnation pressure coefficient
C_{PL}	Lower surface pressure coefficient $= (p_L - p_\infty)/\frac{1}{2}\rho_\infty V_\infty^2$
C_{PU}	Upper surface pressure coefficient $= (p_u - p_\infty)/\frac{1}{2}\rho_\infty V_\infty^2$
d	Local water depth at model surface
d_∞	Undisturbed water depth
M_a	Local Mach Number in air
M_W	Local "water Mach Number", i.e. when $\gamma = 2$
$M_{W\infty}$	Freestream "water Mach Number"
M_∞	Freestream Mach Number
$M_{a\infty}$	Freestream Mach Number when a clear distinction is needed that $\gamma = 1.4$
p	Local pressure
p_L	Local pressure on lower surface
p_U	Local pressure on upper surface
p_∞	Freestream pressure
p_o	Stagnation pressure
t	Semi-thickness of wedge section at the shoulder
V	Carriage speed, or model speed
V_∞	Freestream air velocity
x	Wedge chordwise co-ordinate
y	Vertical distance on model side between water surface and apparent bottom of model

List of Symbols (Continued)

α	Wedge angle of incidence
γ	Ratio of the specific heats
ξ_∞	Transonic similarity parameter (see below)
θ	Wedge semi-angle, approx. equal to t/c
ϕ	Perturbation velocity potential
ρ_∞	Freestream air density

Generalized coefficients in Transonic similarity form

$$\tilde{\alpha} = \frac{\alpha}{t/c}$$

$$\tilde{C}_{Do} = \frac{\left[M_\infty^2(\gamma+1)\right]^{\frac{1}{3}}}{(t/c)^{5/3}} C_{Do}$$

$$\tilde{C}_L = \frac{\left[M_\infty^2(\gamma+1)\right]^{\frac{1}{3}}}{(t/c)^{2/3}} C_L$$

$$\tilde{C}_P = \frac{\left[M_\infty^2(\gamma+1)\right]^{\frac{1}{3}}}{(t/c)^{2/3}} C_P$$

$$\widetilde{\left(\frac{dC_L}{d\alpha}\right)} = \left[M_\infty^2(\gamma+1)(t/c)\right]^{\frac{1}{3}} \left(\frac{dC_L}{d\alpha}\right)_{\alpha=0}$$

$$\widetilde{\left(\frac{\Delta C_P}{\alpha}\right)} = \frac{\tilde{C}_{PL} - \tilde{C}_{Pu}}{\alpha}$$

$$\xi_\infty = \frac{M_\infty^2 - 1}{\left[M_\infty^2(\gamma+1)(t/c)\right]^{2/3}}$$

1. Introduction

The similarity between the differential equations of the transonic flow of a gas in two dimensions and for the flow of shallow water has led to the investigation of the latter as a cheap alternative to transonic wind tunnels. The original suggestion came from Jouguet[1] (1920) and much work has been done in this connection since about 1940.

The work of a number of other investigators has been drawn upon to decide the following conditions for this experimental programme :-

(i) Single wedge sections have been used, as the front halves of diamond sections, on the assumption that the sonic line leaves the surface of the latter at the shoulder, so that conditions in front of and behind the shoulder can be taken as independent, there being moreover a favourable pressure gradient on the front wedge. Hence boundary layer, and therefore Reynolds number, effects will be small and boundary layer separations will be avoided. Furthermore, much theoretical and experimental data are available for wedge sections, single and double.

(ii) A depth of one quarter inch is used on the basis of the papers of Laitone[2][3], We jers[4] and others, to the effect that this depth gives the best approximation of the group velocity to the wave velocity, which, in turn, tends to the value $(gd_\infty)^{\frac{1}{2}}$ independent of wave length, except for very small capillary waves, where d is the undisturbed water depth.

(iii) The model size of 6 inch chord was chosen to generate waves of the longest convenient length[2][5] for the tank which was 4 feet wide.

(iv) The effect of bottom clearance between model and tank has been kept to a minimum consistent with the free movement of the carriage and was checked by tests on the 20° wedge at 7° incidence.

The present programme follows various exploratory investigations carried out over the last few years, by students at the College of Aeronautics, on aerofoil shapes and wedges[6][7][8]. This report aims to give a systematic account of the apparatus, test technique, reduction of results, and the overall accuracy of the College of Aeronautics apparatus and method, together with a comparison with theory and with other existing experimental results.

The final results for wedges of total nose angle 10°, 15° and 20° include the variation of the lift and drag coefficients with angle of incidence and with Mach Number, plotted in the generalized transonic forms of these quantities.

Errors of the order of 100% on the smallest quantities are possible with this apparatus, although the integrated results do not appear to have been greatly in error. The question of experimental error is dealt with in Appendix 3. A number of readings which showed considerable departures from the best curves through the experimental points were rejected.

The analogy on which the experimental work was based has the drawback that a gas having $\gamma = 2.0$ is implied by the hydrodynamic equations. The change to $\gamma = 1.4$ can be carried out by applying von Doenhoff's method developed for Freon-12, but, perhaps, more accurately by the use of transonic similarity forms.

2. Hydraulic Analogy

The water analogy on which this investigation is based can be briefly described as follows. The full form of the equations for the transonic flow of a gas are intractable and the usual assumption is made that there are only small perturbations of velocity from the free stream value.

Neglecting terms higher than the second order, the potential equation of motion reduces to

$$(1 - M_\infty^2)\ \phi_{xx} + \phi_{yy} + \phi_{zz} = M_\infty^2 \left[\frac{\gamma + 1}{V_\infty}\ \phi_x\ \phi_{xx} + \frac{\gamma - 1}{V_\infty}\ .\ \phi_x\ (\phi_{yy} + \phi_{zz}) + \frac{2}{V_\infty}\ (\phi_y\ \phi_{xy} + \phi_z\ \phi_{xz}) \right] \qquad (1)$$

where ϕ is the perturbation velocity potential; the subscripts refer to differentiation with respect to x, y, z; V_∞ is the free stream air velocity; and M_∞ is the free stream Mach number. When ϕ_x, ϕ_y, ϕ_z are small compared with V_∞ and $M_\infty^2 << 1$, this equation (1) reduces to the Prandtl-Glauert equation

$$(1 - M_\infty^2)\ \phi_{xx} + \phi_{yy} + \phi_{zz} = 0 \qquad (2)$$

This, however, is not sufficiently accurate for transonic flow analysis. As M_∞ tends to unity $\dfrac{M_\infty^2 (\gamma + 1) \phi_x}{V_\infty}$ and $(1 - M_\infty^2)$ are of a similar order of magnitude, so the first non-linear term of equation (1) must be retained to give

$$(1 - M_\infty^2)\ \phi_{xx} + \phi_{yy} + \phi_{zz} = \frac{M_\infty^2}{V_\infty} (\gamma + 1)\ \phi_x\ \phi_{xx} \qquad (3)$$

an equation which is tractable at $M_\infty = 1$.

Von Karman[9] introduced a transonic similarity parameter, called here ξ_∞, used since by Kaplan[10] and Spreiter[11]. The form proposed by the latter, using the form of eq.(3) as here derived,

$$\xi_\infty = \frac{M_\infty^2 - 1}{\left[M_\infty^2 \, (\gamma + 1)(t/c)\right]^{\frac{2}{3}}} \tag{4}$$

has been found to give the best correlation between theory and existing experimental data and has received widespread support since its inception. Here t is the semi-thickness of the wedge at the shoulder and c is the wedge chord length.

Kaplan[10] writes as follows :

"If a series of bodies having the same distribution function $g(x/c)$ for the slope, but different thickness ratios (t/c), are placed in flows of different freestream Mach Numbers M_∞ and different values of γ, such that the parameter ξ_∞ (as defined above) remains constant, then the flow patterns are similar in the sense that the same function $f(x/c,\ y/c)$ describes the flow".

We now look at the direct hydraulic analogy which forms the basis of the experimental work described in this paper. The diagrams (a) and (b) are for a two dimensional gas flow and for a heavy inviscid liquid.

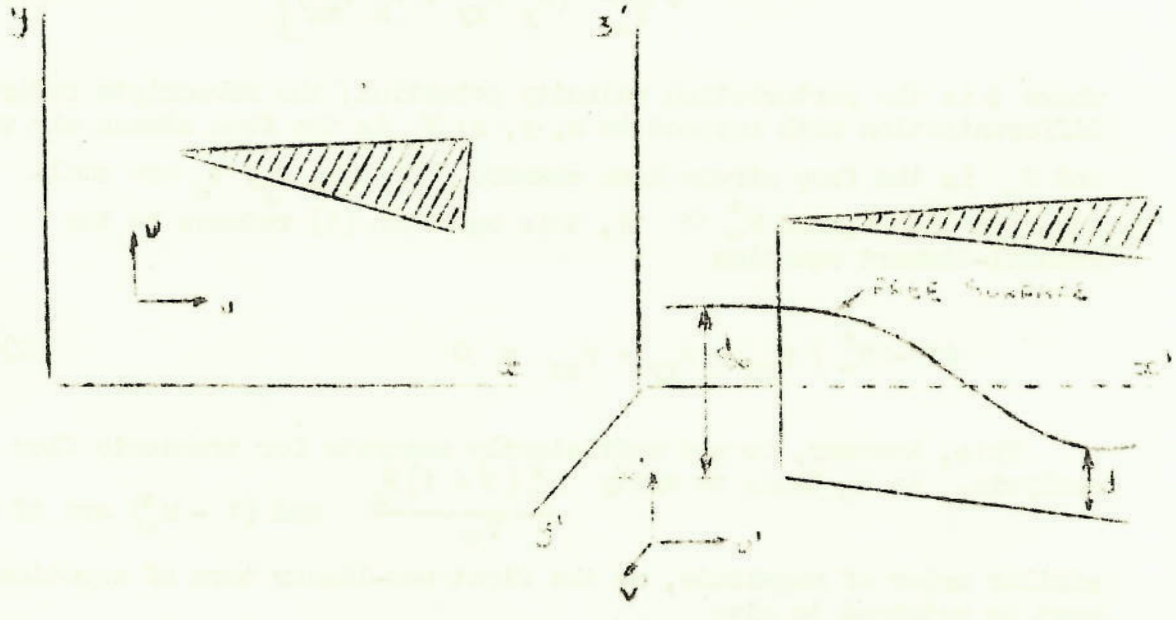

(a) xy-plane for a two-dimensional gas flow

(b) xz-plane for a heavy inviscid liquid

The equations for two-dimensional isentropic flow of a gas are

$$\begin{aligned}
&\frac{\partial}{\partial x}(\rho u) + \frac{\partial}{\partial y}(\rho v) + \frac{\partial \rho}{\partial t} = 0 \\
&u\frac{\partial u}{\partial x} + v\frac{\partial u}{\partial y} + \frac{\partial u}{\partial t} = -\frac{1}{\rho}\frac{\partial p}{\partial x} = -\frac{1}{\gamma - 1}\frac{\partial}{\partial x}(a^2) \\
&u\frac{\partial v}{\partial x} + v\frac{\partial v}{\partial y} + \frac{\partial v}{\partial t} = -\frac{1}{\rho}\frac{\partial p}{\partial y} = -\frac{1}{\gamma - 1}\frac{\partial}{\partial y}(a^2)
\end{aligned} \tag{5}$$

It can be shown(6)(13) that the equations for long surface waves in shallow heavy inviscid liquid, over a plane horizontal bottom, bounded by vertical walls, and in which vertical accelerations and surface tension are negligible, are

$$\begin{aligned}
&\frac{\partial}{\partial x'}(u'd) + \frac{\partial}{\partial y'}(v'd) + \frac{\partial d}{\partial t} = 0 \\
&u'\frac{\partial u'}{\partial x'} + v'\frac{\partial u'}{\partial y'} + \frac{\partial u'}{\partial t} = -\frac{\partial}{\partial x'}(gd) \\
&u'\frac{\partial v'}{\partial x'} + v'\frac{\partial v'}{\partial y'} + \frac{\partial v'}{\partial t} = -\frac{\partial}{\partial y'}(gd)
\end{aligned} \tag{6}$$

The two sets of equations (5) and (6) represent the same type of flow, provided that there is simultaneous correspondence between d and ρ; gd and a^2; γ and 2.

Furthermore, for long waves in shallow water, where d_∞ is the undisturbed depth, Wave group velocity $\rightarrow$ Wave velocity $\rightarrow (gd_\infty)^{\frac{1}{2}}$

There is, then, a correspondence between

$$\frac{V}{(gd_\infty)^{\frac{1}{2}}} \quad \text{and } M_\infty$$

where M_∞ is the free stream Mach number.

Laitone(2) has shown that, with a judicious choice of water depth (about $\frac{1}{4}$ inch), this analogy is still applicable when the wavelength is as small as one inch.

We have, then the following table of corresponding quantities on which the hydraulic analogy to the isentropic flow of a gas is based :-

Isentropic Gas Flow	Long Waves in Shallow Water
$\frac{\rho}{\rho_\infty}$	$\frac{d}{d_\infty}$
$\frac{T}{T_\infty}$	$\frac{d}{d_\infty}$
$\frac{p}{p_\infty}$	$\left(\frac{d}{d_\infty}\right)^2$
a^2	gd
$\frac{u}{a}$	$\frac{u}{(gd)^{\frac{1}{2}}}$

The above analysis makes two assumptions which are, in practice, quite justified, namely, that vertical accelerations in the water can be neglected and that surface tension is negligible. The analogy can also not be extended to deal with viscous effects in the fluid, which effects occur in the present experiments only in the boundary layer of the model and are known to be small. There is the additional restriction that γ is assumed to have the value 2 which differs from that of most gases, air being 1.4.

3. Apparatus

Photographs of the apparatus are given in Figs. 1 and 2. This consisted of arrangements for towing the wedge-shaped models in a water table, 4 feet wide and 6 feet long with a slate bottom that was checked to be horizontal to within 0.001 inch along the centre line before the commencement of this series of tests. The depth of water used throughout the tests was 0.25 inch; this has been shown to be the optimum by Laitone(2)(3), and others. At each filling a calculated volume of water was dispensed from two marked buckets. It was consistently found that the water depth obtained by this method was always 0.25 inch to within the degree of accuracy of the photographic depth measuring technique (see Appendix 3).

The model was moved through the water by means of a cantilever carriage, running on accurately aligned rails, to which it was attached by means of a central spigot and two vertical studs, the latter enabling clearance adjustments to be made. The carriage was activated through a chain drive by an A.C electric motor, and its speed adjusted by varying the brush positions within the motor. The incidence of the model was set by the angular positioning of the central spigot whilst the side of the model was aligned, by means of a three-foot straight edge, with marks scribed on the table; this enabled the incidence to be set to $\pm \frac{1}{10}$ degree.

In the depth measuring technique a photograph was taken of the model in the course of its passage through the water, by a camera moving with the model and an analysis of the apparent depth of the model bottom below a scribed datum line was made at selected chordwise stations. The camera, a Voigtlander Vito 35 mm. fitted with a supplementary lens, was mounted on a platform on an extension of the model carriage in one of the alternative positions shown in Fig. 1, it being necessary always to ensure that the film and the model surface being photographed were parallel in the horizontal plane. In practice, it was found possible to use unique values of the horizontal distance from model side to camera of 13.6 inches and vertical distance of 4.70 inches from tank bottom to centre of camera lens without any significant loss of accuracy.

The film used in the early stages of this work was Pan.X, but it was found that the improved grain properties of Pan.F enabled the projected film to be analysed more easily and that the lower emulsion speed presented no difficulty. With an illumination of 9 x 275 watt Photolita bulbs at approximately 5 feet, and using Pan.F film, an exposure of 1/50th second at f8 gave good results and was used for most of the tests.

The models, each of 6 inches chord, were made of wood with a thin coating of white enamel paint. As can be seen in Fig. 3 (and others) a thin horizontal line is scribed near the top of each model and the chordwise stations are similarly marked. The three models used were single wedge sections of 10°, 15° and 20° included angle. The model leading edges were made as sharp as the use of wood allowed, and the painting of the surfaces rounded off any initial bluntness to an indefinite radius. The leading edge thicknesses were measured with a micrometer gauge and found to be

0.020 inch for the 20° wedge
0.012 inch " " 15° wedge
and 0.005 inch " " 10° wedge,

and this limitation on "sharp leading edge" must be borne in mind when assessing the results.

The speed of the carriage driven through chains and sprocket wheels was recorded during each run by a revolution counting tachometer (see Fig. 1).

4. Test Procedure

After mounting the model on the carriage, the angle of incidence was set andthe bottom clearance was adjusted to the appropriate value (0.010 inch in the main tests) by means of the vertical adjusting screws. From the photographs such as Fig. 3 the amount of the camera tilt was obtained and was found to be invariant with respect to model, incidence, and camera position, within the limits of the accuracy of measurement from the projected photograph. A still phorograph was taken at the start of a series of runs to provide a periodical check of the water depth of a quarter of an inch.

Bomelburg(16) and Bryant(17) have drawn attention to the difficulties arising from dust on the water surface, the latter having overcome the problem by mechanical surface sweeping, whereas the former finally adopted kerosene as the working fluid. Water was retained for the experiments described in this report, and great care was continually exercised to reduce the effect of dust contamination to a minimum; moreover, no given filling of water was ever used for longer than one hour, whilst at each quarter hour the water surface was swept by a three-foot metal straight edge.

One of the weaknesses of the apparatus used was the method of speed regulation which was by the adjustment of the brush positions in the electric motor. The chain wheel by which the brush positions were adjusted (see Fig. 1) did not lend itself to accurate calibration; thus each test run was carried out at a speed which was only approximately known until the reading of the tachometer was taken. This meant in particular that, without extending the tests to a very large number of runs for each setting of the models, it was not possible to ensure that the upper and lower surfaces of a model at a given incidence were photographed at the identical set of Mach Numbers, thus necessitating the plots such as Fig. 4 for the 15° wedge. However, with a given estimated speed setting, the model was photographed in its run at the optimum position as determined by Willmer(8), and the tachometer reading taken, from which the true carriage speed and Mach Number were derived.

After the development of the film, on each one of which some 36 runs were recorded, it was projected onto a screen of white drawing paper to give a magnification of 5 x model full size, the magnification being kept constant so that its factor could be incorporated in the reduction formulae. From the projected image of each run the values of the apparent depth of the model bottom below the datum line were measured at the eleven marked chordwise stations and subsequently analysed.

5. Results

(1) The effect of bottom clearance on the integral of the pressure coefficient $\int_0^1 C_p \, d\left(\frac{x}{c}\right)$ (see Appendix 1) is depicted in Fig. 5, from which it can be seen that, over the complete incidence range of the tests, there is no decisive trend. As a result of this it was considered that no extrapolation to zero clearance was necessary in the subsequent work.

(2) Figs. 6 and 7 give typical results for the Generalized Drag Coefficients plotted against the Transonic Similarity Parameter for constant values of the Generalized Angle of Incidence. The best curves through these and similar plots for other values of α are collected together in Fig. 8.

(3) Figs. 9 to 11 give the Generalized Lift Coefficients plotted against the Transonic Similarity Parameter for constant values of the Generalized Angle of Incidence. The best curves through these plots are collected together in Fig. 12.

(4) Fig. 13 shows the variation of Lift Curve Slope at Zero Incidence in Generalized Form with the Transonic Similarity Parameter, together with the curve given by Transonic Small Disturbance Theory.

(5) Fig. 14 gives the Generalized Pressure Coefficient distribution along the chordline at Zero Incidence.

(6) Fig. 15 gives the Generalized Pressure Coefficient distribution along the chordline due to Incidence.

(7) The overall accuracy of the apparatus is analysed in the figures of Table 6 and in Appendix 3.

6. Discussion

6.1. Effects of bottom clearance

In view of the work of Weijers(14) on the effect of bottom clearance using a static model, the main test programme was preceded by a similar investigation for our case with a moving model. Since the integral of the pressure $\int_0^1 C_p d\left(\frac{x}{c}\right)$ is the basis of all subsequent calculations it was considered a suitable criterion for this test. Further, due to the pressure difference induced across the model by incidence, it was thought that the effect of clearance would be most marked at maximum incidence.

The results for the 20° wedge at 7° incidence and zero incidence, as plotted in Fig. 5, show no decisive trend on which an extrapolation to zero clearance could be based. A convenient working clearance of 0.010 inch was, therefore, adopted for the remainder of the programme.

6.2. The lift results

The generalized lift curve slopes (see Fig. 13) differ substantially from the theoretical curve of Transonic theory. Not only are the experimental points markedly lower than theory predicts, but there is also no tendency for the values to increase with increase of Mach Number.

The results for the 20° wedge differ most widely from the theoretical curve, but tend to increase with the transonic similarity parameter. The results for the other two wedges show a reasonable agreement for values of the transonic similarity parameter less than 0.6.

Upon examination of Figs. 9 to 11 it is again apparent that the results for the 20° wedge depart most widely from the mean.

6.3. The drag results

The zero incidence generalized drag coefficient results for the 10° and 15° wedges agree well with the curve for transonic theory (see Fig. 6), but those for the 20° wedge are all somewhat high, contrary to the findings of Willmer(8). The effect of incidence on drag is shown in Fig. 8, and it is noteworthy that the curves for $\tilde{C}_D$ against ξ_∞ for increasing values of $\tilde{\alpha}$ have precisely the same shape as that for zero incidence given by theory and that they accord well with it. The peak values for drag, it will be noted, occur at progressively lower values of transonic similarity parameter as the generalized incidence increases. At the present time there are no published results showing the variation of the generalized drag curve with incidence with which to compare these curves, and, regarding these curves it must be remembered that they are derived from rather scattered evidence such as Fig. 7.

The wind tunnel study of Liepmann and Bryson(24) is of considerable interest in relation to Fig. 8. Their results given in Fig. 14 of the above reference have been meaned for plotting in Fig. 16 for $\tilde{C}_D$ against ξ_∞ over a range for the latter variable from -1.0 to nearly 3.0, together with the theoretical curves for shock expansion and linear theories. Over the range of the College of Aeronautics experiments up to just past Mach 1, the agreement in trend with the former theory is good. The results for linear theory are also given in Fig. 16 for the higher Mach numbers showing a trend over that range - mainly beyond the College experiments - of the same nature as that for shock expansion theory.

6.4. The generalized pressure distributions

The zero incidence generalized pressure distribution, as plotted in Fig. 14, shows the same general shape as the theoretical curves given by Cincenti and Wagoner[19] and Guderley and Yoshihara[20]. Careful study of the experimental points shows that $\tilde{C}_p$ at a given chordwise station increases with transonic similarity parameter, but not to the extent predicted. This, no doubt, explains the discrepancy between the experimental and theoretical values of $\left(\frac{dC_L}{d\alpha}\right)$ at the approach of shock attachment.

Also given in Fig. 14 is an experimental curve of generalized pressure distribution for $\xi_\infty = 0.74$ obtained by Fleddermann and Stancil[21] using a similar apparatus to the one under discussion but measuring water depth by means of surface contact probes. This curve is included for the purposes of comparison - it will be noticed that the form of pressure variation departs significantly from the theoretical, although, broadly speaking, a closer approximation in magnitude is achieved compared with thsi present investigation.

The distribution of the loading per unit angle of incidence over the chord is shown in generalized form in Fig. 15. Also included in this figure are curves given by transonic small disturbance theory as calculated by Vincenti and Wagoner[22] and Guderley and Yoshihara[23] for particular values of the similarity parameter. Only qualitative agreement with the theoretical curves can be claimed for the experimental points, in that the values of $\left(\frac{\Delta\tilde{C}_P}{\alpha}\right)$ are high at the leading edge and low at the shoulder, and are of the same order around mid-chord; the experimental points tend to be low at the leading edge and high at the trailing edge. It is possible to detect a tendency for the local values of $\left(\frac{\Delta C_P}{\alpha}\right)$ to increase with ξ_∞ (as predicted by the theory) but with insufficient consistency to enable a set of experimental curves to be drawn.

In assessing the results shown in Fig. 15 it should be borne in mind that, due to the large possible errors of this apparatus (see Appendix 3), the pressure distributions for the higher angles of incidence for each wedge were chosen for reduction in the hope of minimising their possible effects.

6.5. General

Because of the method of measurement no depth readings could be obtained near the nose and shoulder of the wedges; the extent of both these regions is of the order of 10% of the chord, although at the higher Mach Numbers and angles of incidence up to 20% of the chord at the leading edge may be affected. Thus, in order to obtain

$$\int_0^1 C_{P_{L(u)}} \, d\left(\frac{x}{c}\right)$$ it was necessary to assume that :-

(a) The stagnation pressure coefficient was that given by theory (see Fig. 17), and that the stagnation point was at the leading edge.

(b) A leading edge separation bubble was produced on the upper surfaces of the wedges at incidence, and that when no clear indication was given in the readings, the pressure coefficient was taken as constant from the leading edge to the first reliable value.

(c) There is always a Mach Number of unity at the shoulder.

The validity of these assumptions is doubtful, but they are essential in the absence of information about flow conditions in the region of the base of single wedge sections. From the majority of C_p values derived it would appear that the full theoretical stagnation pressure coefficient is not developed, possibly due to the water slope near the leading edge. The theoretical stagantion pressure is assumed to be correct so that, in general, the experimental values must be too low, which would help to explain the deficiencies in the final results. The low values may well be due to the effect of water surface slope, as suggested in Appendix 3, as the water surface is certainly depressed along the side of the model and has to regain the value d_∞ in all directions, in particular, laterally, albeit slowly for M_∞ of the order unity.

The presence of a leading edge separation bubble on the upper surface of the wedges at incidence is well shown by Fig. 18, and appears to cover about 10% of the chord.

The most doubtful assumption is (c) above. Bonham-Carter and Butler(7) have discussed this at some length and conclude, as we have found, that the true sonic point moves forward on the upper surface with increasing incidence and Mach Number, but there is no definite information regarding the actual shoulder and base pressures. Vincenti, Dugan and Phelps(14) also confirm this forward movement of the sonic point for diamond sections.

The most important errors in this work arise from the technique of depth measurement (see Appendix 3). Even assuming an horizontal water surface at the point through which the camera views the model bottom, interpretation errors can give rise to pressure coefficient errors of up to 0.2; taking a constant error in C_P of 0.1 the resulting errors in C_L and C_D can approach 100% of the calculated values (see Table 6). As there is some lateral water surface slope at the side of the model, the errors may be even greater (see Appendix 3). An alternative method of depth measurement is essential if the existing apparatus is to be used for more accurate experiments. The writers have been advised that no film exists with a finer grain and yet with sufficient emulsion speed for this type of work; it would appear that the only possible means of improving the existing technique is the use of a larger camera, implying, of course, a larger initial photographic image. This would improve the reading accuracy. Two methods of depth measurement using vertical probes, due to Laitone and Nielson(15) and Fleddermann and Stancil(21), are alternatives; the accuracies of their methods is unknown to the writers.

Bryant(5) has suggested that, in order to establish a complete affinity between the model wedge and the prototype, account should be taken of the presumed boundary layer development. It is possible to approximate to the effect of the boundary layer on the model in the water by carrying out a laminar flow calculation for the displacement thickness at the shoulder, and assuming a linear boundary layer growth from the leading edge. It is appreciated that this is only very approximate; however, following Bryant(18), it is found that, at $M = 1$, the boundary layer has the effect of increasing the wedge semi-angle by about 0.5°. It should prove worth while introducing this boundary layer modification into the analysis of further experiments, but it has not been done in this investigation.

Some photographs have been selected from the numerous test runs. Fig. 19 with the model at rest, illustrates the difficulty of obtaining a uniform meniscus, particularly at the leading and trailing edges and the application of a thin film of weak detergent solution to the model surface before each run gave some improvement. Fig. 20 shows the impossibility of obtaining results near the leading edge, both because of the bow wave effect on the photography and because of the probable breakdown of the analogy due to the appreciable vertical accelerations of the water particles. Capillary waves ahead of the bow wave are also clearly visible. Figs. 3 and 18 show the characteristics depression of the water at the trailing edge which precludes the taking of any readings at the shoulder of the wedge.

Although the possibility of large errors has been shown to exist, there is evidence from the final curves that the effect on the results has been kept within reasonable limits by the extensive range of tests and the effective smoothing of the readings, such as in Fig. 4.

The value of the results rests on the success or failure of the various smoothing operations.

7. Conclusions

(1) Given an accurate depth measuring technique the hydraulic analogy provides a useful method of obtaining data in transonic gas dynamics at low cost, particularly in problems of unsteady flow, provided shock waves are absent.

(2) The College of Aeronautics apparatus, in its present form, is not recommended for the continuance of serious research work, although it would still be useful for routine studen experiments, and for demonstration purposes. The following modifications to the apparatus would, however, make it suitable for further research work :-

(i) The provision of a system of probes for depth measurement to replace the present photographic method.

(ii) The provision of an accurate speed control.

(iii) The stiffening of the model mounting.

(iv) The provision of a drain in a remote corner of the water table to allow the use of alternative working fluids, such as kerosene.

(3) Within the degree of accuracy of these experiments it is concluded that :-

(i) The generalized results for the 10° and 15° wedges follow the trends predicted by transonic small disturbance theory, although the absolute values at incidence tend to be low and agree with the trends obtained by other workers in wind tunnel tests.

(ii) The results for the 20° wedge indicate that a semi-nose angle of 10° is too large for the application either of transonic small disturbance theory or of the hydraulic analogy, as might be expected at high lift coefficients.

Acknowledgement

The authors wish to express their thanks for the assistance of their supervisors, Mr. G.M.Lilley and Mr. W.J.Rainbird.

8. References

1. Jouguet, E. Some Problems in General Hydrodynamics. Journal de Mathematiques Pures et Appliquees, (Series 8) Vol.3.1., 1920.

2. Laitone, E.V. A Study of Transonic Gas Dynamics by the Hydraulic Analogy. Journ. Aero. Sci. Vol.19, No.4 April, 1952.

3. Laitone, E.V. A Rational Discussion of the Hydraulic Analogy. Jour. Aero. Sci. Vol.20, No.1 Jan.1953.

4. Weijers, P.F.R. The Use of a Shallow Water Channel for Quantitative Investigation of Compressible Gas Flow. Aero. Res. Labs. (Aust.), Aero. Note No.123.

5. Bryant, R.A.A. The Hydraulic Analogy as a Distorted Dissimilar Model. Jour. Aero. Sci. Vol.23, No.3, March 1956.

6. Sandford, J. The Determination of the Pressure Distribution Round an Aerofoil in Transonic Gas Flow Using the Hydraulic Analogy. College of Aeronautics Thesis, June 1954.

7. Butler, D.C., Bonham-Carter, G.E.D. Transonic Flow Past Wedge Profiles by Hydraulic Analogy. College of Aeronautics Thesis, June 1955.

8. Willmer, M.A.P. Transonic Results for Lifting and Non-Lifting Wedges using the Hydraulic Analogy. College of Aeronautics Thesis, June 1956.

9. Von Karman, T. Supersonic Aerodynamics - Principles and Applications. Jour. Aero. Sci. Vol.14, No. 7 July 1947.

10. Kaplan, C. On Similarity Rules for Transonic Flows. N.A.C.A. Report No. 894, 1948.

11. Spreiter, J.R. On the Application of Transonic Similarity Rules to Wings of Finite Span. N.A.C.A. Report No. 1153, 1953.

References (Continued)

12. Von Doenhoff, A.E., Braslow, A.L., Schwartzberg, M.A. — Studies of the Use of Freon-12 as a Testing Medium in the Langley Low Turbulence Tunnel. N.A.C.A. T.N.3000, August, 1953.

good for waves

13. Lamb, Sir Horace — Hydrodynamics. 6th Edition C.U.P., Chap. 9, 1932.

14. Vincenti, W.G., Dugan, D.W., Phelps, E.R. — An Experimental Study of the Lift and Pressure Distribution on a Double-Wedge Profile at Mach Numbers near Shock Attachment. N.A.C.A. T.N.3225, July, 1954.

15. Laitone, E.V., Nielson, H. — Transonic Flow Past Wedge Profiles by Hydraulic Analogy. Jour. Aero. Sci. Vol.21, No.7, July 1954.

16. Bomelburg, H.J. — Comment on "Wedge Pressure Coefficients in Transonic Flow by Hydraulic Analogy". Jour. Aero. Sci., Vol.22 No. 10, October, 1955.

no useful info

17. Bryant, R.A.A. — Some Comments on Surface Contamination in Hydraulic Analogy Research. Jour. Aero. Sci. Vol.23, No.11, November, 1956.

18. Bryant, R.A.A. — The Size of Aerofoil Models for Quantitative Hydraulic Analogy Research. Jour. Royal Aero. Soc. Vol.60, No.543, March, 1956.

19. Vincenti, W.G., Wagoner, C.B. — Transonic Flow Past a Wedge Profile with Detached Bow Wave - General Analytical Method and Final Calculated Results. N.A.C.A. T.N.2339, April 1951.

20 Guderley, G., Yoshihara, H. — The Flow Over a Wedge Profile at Mach Number 1. Jour. Aero. Sci. Vol.17, No.11, November, 1950.

21. Fleddermann, R.G., Stancil, R.T. — Wedge Pressure Coefficients in Transonic Flow by Hydraulic Analogy. Jour, Aero. Sci., Vol.22, No.4 April, 1954.

22. Vincenti, W.G., Wagoner, C.B. — Theoretical Study of the Transonic Lift of a Double-Wedge Profile with Detached Bow Wave. N.A.C.A. Report No.1180, 1954.

References (Continued)

23.	Guderley, G., Yoshihara, H.	Two-Dimensional Unsymmetrical Flow Patterns at Mach Number 1. Jour. Aero. Sci. Vol.20, No.11, Nov.1953.
24.	Liepmann, H.W., Bryson, A.E.	Transonic Flow Past Wedge Sections. Jour. Aero. Sci. Vol.17, No.12, Dec.1950.

APPENDIX 1

REDUCTION OF RESULTS

The water depths d and d_∞ and the vertical distance D between the model bottom and model datum were calculated from known data and from measurements of the photographic film. A chart was prepared for determining local values of M_W ($\gamma = 2$) from local depth ratios and free stream $M_{W\infty}$ and another for determining local pressure coefficients from local Mach numbers and freestream Mach numbers in air ($\gamma = 1.4$). The realtionship between local water Mach number M_W and local air Mach number M_a for the variation of thickness/chord ratio with the freestream Mach number $M_{a\infty}$ ($\gamma = 1.4$) was plotted. Tables were then constructed for the three wedges of 10°, 15° and 20° as shown in the sample tables for the 15° wedge. Thus the integral of the pressure measured along the wedge was obtained in Table 1. Fig. 17 gives the variation of stagnation pressure coefficient with freestream Mach number. The results of the calculation of transonic similarity parameter factors are given in Table 2. These last lead to the calculation of lift and drag and thus to the parameters $\tilde{C}_{Do}$ and $\tilde{C}_L$, again shown in tabulated form in Table 3 for the 15° wedge. Typical results of $\tilde{C}_D$ for this wedge angle are given in Table 4 and in Figs. 6 and 7 for all three wedge angles at zero incidence and at $\tilde{\alpha} = 0.1$ to show the experimental scatter; the faired curves in Fig. 8 are for the complete range of angle. Figs. 9 - 12 give the results for the generalised lift coefficient $\tilde{C}_L$ plotted against the transonic similarity parameter ξ_∞. The calculations of the lift slope lead to Fig. 13, where a comparison is made with theory. The values of $\tilde{C}_{P_{u(L)}}$, the zero incidence chordwise generalised pressure coefficient distribution along the chord are calculated in Table 8 for the wedge of 15° and are compared with theory in Fig. 14 for a range of values of the parameter ξ_∞. This is followed by the chordwise lift distribution in Fig. 15

APPENDIX 2

(1) CONVERSION OF 'WATER MACH NUMBERS' TO THE CORRESPONDING 'AIR MACH NUMBERS'

(2) VARIATION OF THICKNESS FACTOR WITH MACH NUMBER

(1) For streamline-similarity, that is for the ratio of stream tube areas to be the same in both water and air at corresponding points it is shown by von Doenhoff (N.A.C.A. T.N.3000) that

$$M_w \left[\frac{1 + \frac{\gamma_w - 1}{2} M_w^2}{\frac{\gamma_w + 1}{2}} \right]^{-\frac{\gamma_w + 1}{2(\gamma_w - 1)}} = M_a \left[\frac{1 + \frac{\gamma_a - 1}{2} M_a^2}{\frac{\gamma_a + 1}{2}} \right]^{-\frac{\gamma_a + 1}{2(\gamma_a - 1)}} \qquad (1)$$

where suffixes w and a refer to water and air respectively.

Substitute $\gamma_w = 2 \quad \gamma_a = 1.4$ whence

$$M_w \left(\frac{2 + M_w^2}{3} \right)^{-\frac{3}{2}} = M_a \left(\frac{5 + M_a^2}{6} \right)^{-3}$$

Square both sides and invert, whence

$$\frac{\left[12 \; (2 + M_w^2) \right]^3}{M_w^2} = \frac{\left[5 + M_a^2 \right]^6}{M_a^2} \qquad (2)$$

(2) Equating corresponding values of ξ_∞ for air and water

$$\frac{M_{a\infty}^2 - 1}{\left[(\gamma_a + 1)(\frac{t}{c})_a \, M_{a\infty}^2 \right]^{\frac{2}{3}}} = \frac{M_{w\infty}^2 - 1}{\left[(\gamma_w + 1)(\frac{t}{c})_w \, M_{w\infty}^2 \right]^{\frac{2}{3}}}$$

$$\frac{(\frac{t}{c})_a}{(\frac{t}{c})_W} = \left(\frac{M^2_{a\infty} - 1}{M^2_{W\infty} - 1}\right)^{\frac{3}{2}} \left(\frac{\gamma_W + 1}{\gamma_a + 1}\right) \left(\frac{M_{W\infty}}{M_{a\infty}}\right)^2$$

$$= 1.25 \left(\frac{M^2_{a\infty} - 1}{M^2_{W\infty} - 1}\right)^{\frac{3}{2}} \left(\frac{M_{W\infty}}{M_{a\infty}}\right)^2$$

$$= 1.25\ f(M_{a\infty})$$

using the relation between $M_{a\infty}$ and $M_{W\infty}$ in equation (2) above.

It is not possible to evaluate $f(M_{a\infty})$ between the values of $M_{a\infty} = 0.95$ and $M_{a_\infty} = 1.05$ owing to the rapid changes in (2). The functions are too complicated to carry out a limiting process by de l'Hopital's rule around $M_{a\infty} = 1$ so values have been interpolated.

The maximum value of the thickness factor in the range $0.9 \leq M_\infty \leq 1.25$ is 1.025 so this factor was not included in the calculations.

APPENDIX 3

EXPERIMENTAL ACCURACY

Error may arise in this experiment from any of the following :-

(1) measurement of carriage speed

(2) incidence setting

(3) bottom clearance

(4) camera position relative to model

(5) vertical alignment of the model

(6) inaccuracy of carriage track and/or non-horizontal tank-bottom

(7) reading errors

(8) incorrect assumptions of the depth measuring technique.

(1) Measurement of carriage speed

It was found that the tachometer gave lower readings for the same power setting when the carriage was engaged than when the chain was running freely. Furthermore, the tachometer needed a longer time to register than the actual runs allowed. Bearing in mind these facts, the repeatability gave an error of up to three in the tachometer r.p.m. which corresponds to an error of 0.01 in the 'water Mach number'.

(2) Incidence setting

The method of incidence setting had an accuracy of $\pm\frac{1}{10}^{\circ}$ with the method used.

(3) Bottom clearance

Several different bottom clearances were tried with the 20° wedge at several incidences and no decisive trend was discovered (see Fig. 7). It was therefore concluded that no small departures from the setting 0.01 in. used throughout the main body of the tests had any effect.

(4) Camera position relative to model

It was found that variation in camera position over the restricted range necessary gave only very small percentage differences in the constants used in the depth measurement.

(5) Vertical alignment of the model

It was found difficult to assure that the bottom clearance was the same at both sides of the model. This part of the apparatus could definitely be made more rigid as even when the correct adjustment had been made there was still a fair amount of spring.

(6) Inaccuracy of carriage track and/or non-horizontal tank-bottom

The tank-bottom had been checked as being horizontal to within 0.001" along the centre line, but an exhaustive check of bottom, drive rails, etc. was not made.

(7) Reading errors

It was found that the error in the reading of height on the 5x full size screen picture was ± 0.02", whether the reading was repeated by the same or another person. Six cases were treated covering the usable range and at extreme Mach numbers. The whole calculation was carried through to the end-results of C_L and C_{D_o} and is tabulated in Table 6.

(8) The photographic depth measuring technique relied explicitly on the water surface being horizontal at the point of incidence. No attempt has heretofore been made to assess the possible error in this assumption. The error variation for deviations of θ from zero is tabulated below. It may be shown that lateral pressure recovery is extremely slow and that the water-slope should be correspondingly low. This is a point which could bear experimental investigation.

θ	0	5	10	15
d	0.273	0.239	0.214	0.195
% ERROR	0	12.5	21.6	28.6
C_P at $M_{W\infty}=0.95$	0.240	-0.145	-0.370	
ΔC_P	0	0.385	0.610	
% ERROR	0	161	254	

$$A = \int_0^1 C_p \, d\left(\frac{x}{c}\right)$$

TABLE 1 (a)

10 THOU. BOTTOM CLEARANCE 20° WEDGE, C_p DISTRIBUTION

% c	5	10	20	30	40	50	60	70	80	90	95	INCIDENCE (DEGREES)	UPPER OR LOWER SURFACE	M_{a_∞}
a/a_∞	0.86	0.94	0.95	0.98	1.01	1.00	0.98	0.96	0.94	0.90	0.90	0	-	0.96
C_p	-0.27	-0.07	-0.04	-0.02	0.11	0.00	-0.04	-0.02	-0.07	-0.15	-0.15	A	= -0.046	(20 THOU.)
a/a_∞	1.38	1.37	1.36	1.31	1.29	1.26	1.26	1.25	1.24	1.24	1.14	0	-	1.22
C_p	0.63	0.61	0.60	0.52	0.47	0.41	0.41	0.40	0.38	0.38	0.22	A	= 0.390	
a/a_∞	1.36	1.35	1.31	1.28	1.26	1.24	1.23	1.22	1.19	1.16	1.10	0	-	1.17
C_p	0.65	0.62	0.56	0.49	0.46	0.43	0.40	0.38	0.32	0.27	0.19	A	= 0.370	
a/a_∞	1.29	1.29	1.26	1.25	1.24	1.22	1.20	1.19	1.14	1.13	1.07	0	-	1.12
C_p	0.55	0.55	0.49	0.47	0.46	0.40	0.37	0.35	0.24	0.23	0.14	A	= 0.347	
a/a_∞	1.29	1.26	1.25	1.23	1.20	1.19	1.17	1.14	1.12	1.09	1.01	0	-	1.05
C_p	0.62	0.54	0.53	0.46	0.39	0.38	0.32	0.27	0.22	0.15	0.02	A	= 0.304	
a/a_∞	1.25	1.24	1.22	1.19	1.16	1.14	1.14	1.12	1.09	1.04	1.01	0	-	1.00
C_p	0.61	0.58	0.52	0.46	0.36	0.33	0.33	0.28	0.21	0.08	0.02	A	= 0.273	
a/a_∞	1.18	1.18	1.18	1.16	1.14	1.14	1.12	1.08	1.04	1.02	0.97	0	-	0.96
C_p	0.58	0.58	0.58	0.53	0.45	0.45	0.40	0.29	0.20	0.14	-0.02	A	= 0.380	
a/a_∞	1.25	1.25	1.23	1.19	1.17	1.14	1.13	1.08	1.04	1.02	0.98	1	L	1.21
C_p	0.66	0.66	0.61	0.52	0.47	0.38	0.35	0.19	0.10	0.06	-0.05	A	= 0.415	
a/a_∞	1.29	1.26	1.24	1.20	1.19	1.17	1.14	1.13	1.10	1.03	0.98	1	L	1.15
C_p	0.71	0.67	0.61	0.48	0.46	0.41	0.34	0.30	0.23	0.05	-0.07	A	= 0.392	
a/a_∞	1.24	1.22	1.18	1.16	1.16	1.13	1.13	1.12	1.10	1.06	1.00	1	L	1.00
C_p	0.58	0.52	0.44	0.36	0.33	0.30	0.30	0.28	0.24	0.13	0.00	A	= 0.294	
a/a_∞	1.28	1.26	1.24	1.24	1.23	1.20	1.19	1.16	1.13	1.12	1.06	1	L	1.09
C_p	0.59	0.54	0.49	0.49	0.47	0.40	0.37	0.32	0.25	0.23	0.10	A	= 0.352	
a/a_∞	1.14	1.14	1.12	1.10	1.10	1.10	1.06	1.04	1.03	1.02	0.98	1	U	0.97
C_p	0.36	0.36	0.30	0.27	0.27	0.27	0.16	0.11	0.07	0.05	-0.04	A	= 0.200	
a/a_∞	1.13	1.13	1.13	1.13	1.12	1.10	1.10	1.06	1.04	1.02	1.00	1	U	1.00
C_p	0.27	0.27	0.27	0.27	0.26	0.23	0.23	0.12	0.07	0.03	0.00	A	= 0.231	
a/a_∞	1.20	1.19	1.18	1.16	1.16	1.13	1.12	1.12	1.10	1.06	1.02	1	U	1.08
C_p	0.39	0.36	0.35	0.32	0.32	0.25	0.22	0.22	0.18	0.11	0.03	A	= 0.280	
a/a_∞	1.24	1.24	1.24	1.24	1.22	1.20	1.20	1.18	1.14	1.12	1.08	1	U	1.17
C_p	0.41	0.41	0.41	0.41	0.38	0.34	0.34	0.30	0.23	0.20	0.15	A	= 0.326	
a/a_∞	1.31	1.29	1.26	1.25	1.25	1.25	1.25	1.24	1.24	1.22	1.14	1	U	1.23
C_p	0.50	0.46	0.40	0.39	0.39	0.39	0.39	0.37	0.37	0.33	0.22	A	= 0.352	
a/a_∞	1.20	1.20	1.20	1.14	1.14	1.14	1.12	1.09	1.07	1.03	1.01	2	L	0.96
C_p	0.53	0.53	0.53	0.36	0.36	0.36	0.31	0.22	0.18	0.07	0.02	A	= 0.297	
a/a_∞	1.18	1.18	1.23	1.16	1.16	1.16	1.12	1.10	1.08	1.03	1.01	2	L	1.00
C_p	0.44	0.44	0.38	0.36	0.36	0.36	0.28	0.24	0.19	0.05	0.02	A	= 0.318	
a/a_∞	1.29	1.26	1.25	1.24	1.22	1.22	1.19	1.16	1.13	1.08	1.02	2	L	1.09
C_p	0.59	0.53	0.51	0.48	0.43	0.43	0.38	0.31	0.25	0.15	0.05	A	= 0.372	
a/a_∞	1.35	1.31	1.30	1.25	1.25	1.25	1.23	1.18	1.17	1.14	1.08	2	L	1.15
C_p	0.66	0.58	0.55	0.46	0.46	0.46	0.41	0.31	0.30	0.25	0.15	A	= 0.414	
a/a_∞	1.37	1.37	1.34	1.31	1.30	1.28	1.26	1.24	1.23	1.22	1.16	2	L	1.21
C_p	0.61	0.61	0.55	0.52	0.50	0.46	0.43	0.38	0.37	0.34	0.25	A	= 0.449	
a/a_∞	1.25	1.25	1.23	1.19	1.17	1.14	1.13	1.08	1.04	1.02	0.98	2	U	1.25
C_p	0.66	0.66	0.61	0.52	0.47	0.38	0.35	0.19	0.10	0.06	-0.05	A	= 0.415	
a/a_∞	1.30	1.26	1.26	1.24	1.23	1.22	1.17	1.17	1.14	1.13	1.07	2	U	1.20
C_p	0.51	0.43	0.43	0.40	0.37	0.36	0.28	0.28	0.24	0.23	0.11	A	= 0.291	
a/a_∞	1.26	1.25	1.23	1.20	1.19	1.18	1.17	1.14	1.09	1.10	1.03	2	U	1.13
C_p	0.48	0.47	0.42	0.37	0.35	0.33	0.30	0.24	0.17	0.19	0.05	A	= 0.266	
a/a_∞	1.23	1.22	1.20	1.18	1.17	1.16	1.13	1.12	1.10	1.07	1.01	2	U	1.08
C_p	0.45	0.43	0.40	0.36	0.33	0.32	0.24	0.23	0.18	0.14	0.02	A	= 0.240	
a/a_∞	1.20	1.18	1.16	1.13	1.13	1.09	1.09	1.06	1.02	0.98	0.96	2	U	0.99
C_p	0.48	0.42	0.37	0.30	0.30	0.21	0.21	0.14	0.03	-0.06	-0.10	A	= 0.205	

$$A = \int_0^1 C_p \; d\left(\frac{x}{c}\right)$$

TABLE 1 (a)

10 THOU. BOTTOM CLEARANCE 20° WEDGE, C_p DISTRIBUTION

% c	5	10	20	30	40	50	60	70	80	90	95	INCIDENCE (DEGREES)	UPPER OR LOWER SURFACE	$M_{a\infty}$
d/d_∞	1.20	1.17	1.14	1.13	1.12	1.10	1.09	1.07	1.03	1.01	0.98	2	U	0.94
C_p	0.54	0.47	0.38	0.35	0.32	0.26	0.23	0.17	0.08	0.02	−0.05	A = 0.155		
d/d_∞	1.40	1.38	1.35	1.34	1.31	1.30	1.25	1.24	1.24	1.20	1.16	3	L	1.18
C_p	0.72	0.69	0.63	0.62	0.55	0.54	0.44	0.43	0.43	0.35	0.27	A = 0.475		
d/d_∞	1.34	1.32	1.30	1.28	1.26	1.25	1.24	1.20	1.17	1.13	1.09	3	L	1.12
C_p	0.66	0.62	0.58	0.53	0.49	0.47	0.44	0.37	0.30	0.23	0.17	A = 0.431		
d/d_∞	1.25	1.25	1.24	1.24	1.24	1.22	1.22	1.14	1.12	1.04	1.03	3	L	1.04
C_p	0.55	0.55	0.53	0.53	0.53	0.48	0.48	0.31	0.26	0.07	0.06	A = 0.381		
d/d_∞	1.24	1.24	1.22	1.19	1.18	1.14	1.13	1.09	1.08	1.04	1.00	3	L	0.98
C_p	0.59	0.59	0.54	0.46	0.43	0.32	0.30	0.19	0.17	0.07	0.00	A = 0.336		
d/d_∞	1.14	1.14	1.13	1.13	1.12	1.10	1.09	1.04	1.01	1.01	0.97	3	U	0.98
C_p	0.35	0.35	0.32	0.32	0.30	0.25	0.21	0.10	0.02	0.02	−0.07	A = 0.148		
d/d_∞	1.14	1.14	1.14	1.12	1.12	1.10	1.09	1.07	1.03	1.01	0.98	3	U	1.00
C_p	0.33	0.33	0.33	0.28	0.28	0.24	0.21	0.14	0.07	0.03	−0.05	A = 0.165		
d/d_∞	1.17	1.17	1.16	1.14	1.14	1.12	1.12	1.10	1.06	1.03	1.00	3	U	1.03
C_p	0.35	0.35	0.33	0.29	0.29	0.24	0.24	0.19	0.11	0.04	0.00	A = 0.171		
d/d_∞	1.19	1.19	1.18	1.17	1.16	1.13	1.13	1.10	1.08	1.06	1.01	3	U	1.12
C_p	0.35	0.35	0.34	0.30	0.29	0.24	0.24	0.18	0.14	0.10	0.03	A = 0.226		
d/d_∞	1.25	1.25	1.25	1.24	1.23	1.20	1.19	1.16	1.13	1.10	1.10	3	U	1.18
C_p	0.42	0.42	0.42	0.39	0.38	0.33	0.30	0.27	0.22	0.18	0.18	A = 0.155		
d/d_∞	1.26	1.26	1.25	1.23	1.23	1.19	1.17	1.14	1.13	1.12	1.09	3	U	1.23
C_p	0.42	0.42	0.40	0.36	0.36	0.30	0.27	0.23	0.21	0.19	0.15	A = 0.283		
d/d_∞	1.25	1.24	1.23	1.20	1.19	1.14	1.13	1.12	1.10	1.07	1.04	4	L	0.95
C_p	0.08	0.66	0.65	0.56	0.54	0.40	0.36	0.34	0.27	0.22	0.13	A = 0.350		
d/d_∞	1.29	1.26	1.26	1.24	1.22	1.16	1.14	1.13	1.10	1.06	1.02	4	L	0.99
C_p	0.70	0.65	0.65	0.60	0.53	0.37	0.32	0.30	0.23	0.12	0.03	A = 0.388		
d/d_∞	1.35	1.34	1.29	1.28	1.25	1.24	1.22	1.19	1.18	1.14	1.09	4	L	1.04
C_p	0.78	0.76	0.66	0.62	0.55	0.51	0.46	0.39	0.38	0.29	0.14	A = 0.429		
d/d_∞	1.36	1.35	1.34	1.31	1.28	1.26	1.25	1.24	1.23	1.17	1.12	4	L	1.12
C_p	0.71	0.70	0.68	0.61	0.53	0.50	0.47	0.46	0.42	0.30	0.23	A = 0.473		
d/d_∞	1.45	1.41	1.42	1.38	1.36	1.34	1.32	1.28	1.26	1.23	1.19	4	L	1.21
C_p	0.78	0.70	0.72	0.65	0.60	0.57	0.54	0.47	0.43	0.37	0.31	A = 0.554		
d/d_∞	1.47	1.47	1.46	1.43	1.42	1.38	1.36	1.32	1.28	1.25	1.22	4	L	1.24
C_p	0.75	0.75	0.74	0.69	0.67	0.60	0.55	0.51	0.43	0.38	0.34	A =		
d/d_∞	1.19	1.18	1.19	1.17	1.14	1.14	1.13	1.12	1.07	1.03	1.01	4	U	1.18
C_p	0.32	0.30	0.32	0.29	0.23	0.23	0.22	0.20	0.12	0.05	0.02	A = 0.186		
d/d_∞	1.25	1.20	1.20	1.20	1.18	1.14	1.14	1.13	1.09	1.06	1.03	4	U	1.23
C_p	0.39	0.32	0.32	0.32	0.27	0.22	0.22	0.21	0.15	0.08	0.04	A = 0.233		
d/d_∞	1.17	1.16	1.18	1.18	1.16	1.13	1.13	1.13	1.08	1.04	1.02	4	U	1.12
C_p	0.30	0.29	0.34	0.34	0.29	0.23	0.23	0.23	0.14	0.08	0.03	A = 0.177		
d/d_∞	1.10	1.14	1.14	1.14	1.12	1.12	1.08	1.06	1.02	1.00	1.00	4	U	1.06
C_p	0.19	0.27	0.27	0.27	0.21	0.21	0.14	0.10	0.03	0.00	0.00	A = 0.143		
d/d_∞	1.08	1.13	1.10	1.10	1.10	1.08	1.04	1.02	0.98	0.97	0.95	4	U	1.01
C_p	0.16	0.29	0.24	0.24	0.24	0.16	0.08	0.05	−0.05	−0.07	−0.11	A = 0.102		
d/d_∞	1.09	1.09	1.08	1.08	1.08	1.04	1.04	1.02	1.00	0.98	0.94	4	U	0.98
C_p	0.23	0.23	0.19	0.19	0.19	0.17	0.17	0.05	0.00	−0.05	−0.13	A = 0.085		
d/d_∞	1.57	1.54	1.50	1.46	1.45	1.45	1.41	1.40	1.36	1.29	1.28	5	L	1.26
C_p	0.91	0.85	0.76	0.71	0.70	0.70	0.63	0.62	0.56	0.44	0.42	A = 0.574		
d/d_∞	1.46	1.46	1.43	1.38	1.37	1.34	1.31	1.29	1.25	1.23	1.19	5	L	1.19
C_p	0.82	0.82	0.77	0.67	0.64	0.59	0.53	0.48	0.42	0.37	0.31	A = 0.587		
d/d_∞	1.38	1.38	1.36	1.32	1.29	1.26	1.25	1.23	1.20	1.14	1.10	5	L	1.10
C_p	0.78	0.78	0.73	0.65	0.57	0.50	0.47	0.44	0.38	0.26	0.18	A = 0.514		
d/d_∞	1.31	1.28	1.26	1.25	1.25	1.22	1.18	1.14	1.13	1.08	1.07	5	L	1.00
C_p	0.74	0.69	0.63	0.59	0.59	0.50	0.42	0.31	0.29	0.17	0.15	A = 0.435		

TABLE 1 (a)

10 THOU. BOTTOM CLEARANCE 20° WEDGE, C_p DISTRIBUTION

$A = \int_0 C_p \, d(\frac{x}{c})$

% c	5	10	20	30	40	50	60	70	80	90	95	INCIDENCE (DEGREES)	UPPER OR LOWER SURFACE	M_{a_∞}
a/a_∞	1.32	1.31	1.30	1.25	1.24	1.23	1.22	1.19	1.17	1.13	1.09	5	L	0.98
C_p	0.83	0.75	0.72	0.64	0.60	0.57	0.54	0.46	0.41	0.30	0.21	A = 0.422		
a/a_∞	1.10	1.10	1.12	1.12	1.13	1.13	1.12	1.10	1.08	1.07	1.03	5	U	1.25
C_p	0.15	0.15	0.17	0.17	0.18	0.18	0.17	0.15	0.11	0.10	0.03	A = 0.158		
a/a_∞	1.08	1.09	1.13	1.13	1.13	1.13	1.12	1.10	1.08	1.06	1.03	5	U	1.15
C_p	0.15	0.18	0.24	0.24	0.24	0.24	0.23	0.18	0.15	0.11	0.05	A = 0.136		
a/a_∞	1.02	1.10	1.12	1.10	1.08	1.07	1.07	1.04	1.03	1.00	0.98	5	U	1.09
C_p	0.02	0.18	0.22	0.18	0.14	0.13	0.13	0.08	0.05	0.00	-0.04	A = 0.102		
a/a_∞	1.00	1.06	1.08	1.08	1.07	1.06	1.03	1.03	1.02	0.97	0.96	5	U	1.02
C_p	0.00	0.13	0.18	0.18	0.14	0.13	0.06	0.06	0.05	-0.07	-0.08	A = 0.054		
a/a_∞	1.60	1.54	1.52	1.50	1.46	1.43	1.42	1.38	1.35	1.29	1.23	6	L	1.26
C_p	0.98	0.86	0.84	0.78	0.72	0.68	0.65	0.59	0.54	0.46	0.35	A = 0.615		
a/a_∞	1.53	1.52	1.50	1.46	1.42	1.37	1.34	1.30	1.28	1.23	1.17	6	L	1.21
C_p	0.93	0.92	0.87	0.80	0.73	0.63	0.57	0.50	0.47	0.44	0.28	A = 0.637		
a/a_∞	1.41	1.38	1.36	1.36	1.31	1.28	1.25	1.23	1.18	1.13	1.08	6	L	1.08
C_p	0.85	0.81	0.77	0.77	0.65	0.56	0.50	0.46	0.39	0.26	0.18	A = 0.602		
a/a_∞	1.47	1.47	1.47	1.43	1.36	1.35	1.32	1.29	1.25	1.23	1.19	6	L	1.13
C_p	0.90	0.90	0.90	0.83	0.67	0.64	0.59	0.53	0.45	0.42	0.33	A = 0.550		
a/a_∞	1.38	1.37	1.35	1.34	1.31	1.25	1.25	1.23	1.18	1.13	1.08	6	L	1.02
C_p	0.90	0.89	0.82	0.77	0.74	0.56	0.56	0.51	0.39	0.28	0.16	A = 0.494		
a/a_∞	1.34	1.34	1.32	1.28	1.25	1.24	1.23	1.18	1.14	1.09	1.04	6	L	0.99
C_p	0.87	0.87	0.81	0.70	0.64	0.60	0.57	0.44	0.33	0.21	0.08	A = 0.470		
a/a_∞	0.87	0.98	1.03	1.03	1.03	1.02	1.01	1.02	1.01	0.98	0.91	6	U	0.96
C_p	-0.30	-0.04	0.07	0.07	0.07	0.05	0.02	0.05	0.02	-0.04	-0.22	A = -0.028		
a/a_∞	0.88	0.98	1.02	1.02	1.02	1.02	1.02	1.02	1.01	0.98	0.94	6	U	0.99
C_p	-0.27	-0.05	0.03	0.03	0.03	0.03	0.03	0.03	0.02	-0.05	-0.13	A = -0.011		
a/a_∞	0.90	0.97	1.03	1.04	1.04	1.04	1.04	1.03	1.03	1.01	0.97	6	U	1.06
C_p	-0.20	-0.09	0.04	0.08	0.08	0.08	0.08	0.04	0.04	0.01	-0.09	A = 0.019		
a/a_∞	0.98	1.01	1.06	1.07	1.06	1.07	1.07	1.06	1.03	1.03	1.01	6	U	1.14
C_p	-0.05	0.03	0.11	0.14	0.11	0.14	0.14	0.11	0.05	0.05	0.03	A = 0.077		
a/a_∞	1.01	1.02	1.06	1.07	1.06	1.07	1.08	1.07	1.04	1.03	1.02	6	U	1.21
C_p	0.02	0.03	0.10	0.10	0.10	0.10	0.10	0.10	0.06	0.04	0.03	A = 0.098		
a/a_∞	1.08	1.04	1.09	1.09	1.10	1.10	1.09	1.09	1.06	1.03	1.02	6	U	1.25
C_p	0.11	0.11	0.14	0.14	0.15	0.15	0.14	0.14	0.08	0.03	0.02	A = 0.118		
a/a_∞	1.31	1.31	1.26	1.25	1.24	1.23	1.16	1.13	1.10	1.06	1.02	7	L	0.95
C_p	0.86	0.86	0.70	0.67	0.65	0.62	0.42	0.33	0.26	0.16	0.04	A = 0.509		
a/a_∞	1.37	1.36	1.36	1.32	1.28	1.26	1.23	1.22	1.19	1.13	1.07	7	L	1.01
C_p	0.92	0.88	0.88	0.80	0.67	0.62	0.53	0.51	0.43	0.29	0.15	A = 0.559		
a/a_∞	1.38	1.40	1.37	1.35	1.30	1.26	1.24	1.22	1.19	1.14	1.10	7	L	1.07
C_p	0.83	0.83	0.80	0.75	0.64	0.54	0.49	0.44	0.37	0.28	0.19	A = 0.563		
a/a_∞	1.45	1.42	1.40	1.36	1.34	1.31	1.26	1.24	1.22	1.16	1.10	7	L	1.13
C_p	0.87	0.83	0.77	0.71	0.65	0.59	0.48	0.43	0.40	0.29	0.19	A = 0.628		
a/a_∞	1.53	1.51	1.50	1.47	1.43	1.38	1.37	1.34	1.30	1.22	1.19	7	L	1.21
C_p	0.93	0.89	0.87	0.81	0.73	0.65	0.58	0.54	0.50	0.35	0.31	A = 0.672		
a/a_∞	1.58	1.54	1.52	1.48	1.47	1.42	1.37	1.35	1.32	1.25	1.22	7	L	1.25
C_p	0.97	0.88	0.84	0.76	0.75	0.66	0.58	0.54	0.50	0.39	0.34	A = 0.689		
a/a_∞	0.98	1.00	1.04	1.06	1.06	1.07	1.06	1.03	1.03	1.03	1.01	7	U	1.19
C_p	-0.025	0.00	0.04	0.10	0.10	0.11	0.10	0.04	0.04	0.04	0.02	A = 0.059		
a/a_∞	0.88	0.90	0.98	1.00	1.00	1.00	1.00	0.98	1.00	0.98	0.95	7	U	1.13
C_p	-0.21	-0.17	-0.04	0.00	0.00	0.00	0.00	-0.04	0.00	-0.04	-0.09	A = -0.125		
a/a_∞	0.87	0.91	0.97	1.02	1.02	1.02	1.02	1.02	1.01	0.98	0.95	7	U	1.06
C_p	-0.26	-.018	-0.09	0.03	0.03	0.03	0.03	0.03	0.01	-0.05	-0.11	A = -0.043		
a/a_∞	0.85	0.92	0.98	1.00	1.01	1.00	1.00	1.00	0.98	0.96	0.93	7	U	1.01
C_p	-0.33	-0.18	-0.04	0.00	0.02	0.00	0.00	0.00	-0.04	-0.08	-0.17	A = -0.059		

TABLE 1 (b)

10 THOU. BOTTOM CLEARANCE 15° WEDGE, C_p DISTRIBUTION

$A \int_0 C_p \, d(\frac{x}{c})$

% c	5	10	20	30	40	50	60	70	80	90	95	INCIDENCE (DEGREES)	UPPER OR LOWER SURFACE	$M_{a\infty}$
d/d_∞	1.16	1.14	1.10	1.10	1.08	1.04	1.00	1.00	1.00	0.92	0.87	0	-	0.95
C_p	0.42	0.37	0.26	0.26	0.18	0.11	0.00	0.00	0.00	-0.19	-0.30	$\int_0^1 C_p \, d(\frac{x}{c}) = 0.132$		
d/d_∞	1.27	1.19	1.16	1.16	1.11	1.10	1.10	1.08	1.08	1.02	0.91	0	-	1.01
C_p	0.64	0.43	0.36	0.36	0.24	0.22	0.22	0.17	0.17	0.04	-0.19	$\int_0^1 C_p \, d(\frac{x}{c}) = 0.162$		
d/d_∞	1.25	1.23	1.15	1.13	1.11	1.10	1.04	1.04	1.00	0.97	0.93	0	-	1.06
C_p	0.56	0.48	0.30	0.26	0.21	0.19	0.06	0.06	0.00	-0.08	-0.15	$\int_0^1 C_p \, d(\frac{x}{c}) = 0.207$		
d/d_∞	1.28	1.25	1.24	1.19	1.18	1.14	1.11	1.11	1.10	1.08	1.04	0	-	1.14
C_p	0.52	0.48	0.41	0.35	0.32	0.26	0.20	0.20	0.19	0.08	0.03	$\int_0^1 C_p \, d(\frac{x}{c}) = 0.271$		
d/d_∞	1.38	1.27	1.21	1.19	1.18	1.14	1.13	1.13	1.10	1.08	1.05	0	-	1.20
C_p	0.65	0.45	0.34	0.31	0.30	0.23	0.21	0.21	0.17	0.11	0.09	$\int_0^1 C_p \, d(\frac{x}{c}) = 0.272$		
d/d_∞	1.19	1.15	1.13	1.10	1.10	1.06	1.04	1.04	1.02	0.99	0.91	0	-	1.00
d/d_∞	1.24	1.21	1.20	1.16	1.16	1.16	1.12	1.11	1.11	1.05	1.00	5	L	0.94
C_p	0.67	0.58	0.55	0.44	0.44	0.44	0.31	0.29	0.29	0.13	0.00	A = 0.402		
d/d_∞	1.25	1.24	1.22	1.19	1.18	1.16	1.14	1.13	1.11	1.05	1.00	5	L	0.98
C_p	0.64	0.60	0.56	0.46	0.45	0.39	0.35	0.30	0.25	0.10	0.00	A = 0.438		
d/d_∞	1.30	1.29	1.28	1.26	1.25	1.25	1.18	1.18	1.19	1.15	1.09	5	L	1.03
C_p	0.69	0.66	0.64	0.61	0.56	0.56	0.40	0.40	0.41	0.32	0.17	A = 0.502		
d/d_∞	1.35	1.35	1.31	1.30	1.29	1.27	1.23	1.23	1.23	1.19	1.15	5	L	1.13
C_p	0.69	0.69	0.61	0.58	0.56	0.51	0.43	0.43	0.43	0.37	0.27	A = 0.528		
d/d_∞	1.41	1.39	1.36	1.35	1.33	1.30	1.27	1.27	1.24	1.23	1.23	5	L	1.22
C_p	0.68	0.64	0.59	0.57	0.54	0.49	0.43	0.43	0.37	0.35	0.35	A = 0.518		
d/d_∞	1.28	1.26	1.25	1.21	1.19	1.15	1.14	1.14	1.12	1.05	1.02	5	L	1.00
C_p	0.69	0.65	0.61	0.50	0.46	0.35	0.33	0.33	0.28	0.10	0.05	A = 0.469		
d/d_∞	0.96	0.97	0.95	0.97	0.96	0.98	0.98	0.98	0.95	0.88	0.88	5	ν	0.96
C_p	-0.08	-0.07	-0.12	-0.07	-0.08	-0.03	-0.03	-0.03	-0.12	-0.27	-0.27	A = -0.083		
d/d_∞	0.98	0.98	0.98	0.98	0.97	0.97	0.97	0.97	0.98	0.90	0.88	5	U	1.01
C_p	-0.03	-0.03	-0.03	-0.03	-0.07	-0.07	-0.07	-0.07	-0.03	-0.23	-0.26	A = -0.080		
d/d_∞	1.00	1.00	1.00	1.00	1.00	1.00	0.97	1.00	0.98	0.92	0.90	5	U	1.07
C_p	0.00	0.00	0.00	0.00	0.00	0.00	-0.07	0.00	-0.05	-0.16	-0.20	A = -0.050		
d/d_∞	1.00	1.01	1.01	1.01	1.01	1.00	0.98	1.00	0.98	0.90	0.88	5	U	1.12
C_p	0.00	0.02	0.02	0.02	0.02	0.00	-0.04	0.00	-0.04	-0.23	-0.23	A = -0.019		
d/d_∞	1.08	1.03	1.02	1.02	1.02	1.01	0.98	1.00	0.98	0.92	0.90	5	U	1.18
C_p	0.14	0.05	0.03	0.03	0.03	0.01	-0.05	0.00	-0.05	-0.14	-0.19	A = -0.005		
d/d_∞	1.12	1.04	1.00	1.02	1.00	1.00	0.96	0.97	0.97	0.93	0.88	5	U	1.23
C_p	0.19	0.07	0.00	0.03	0.00	0.00	-0.06	-0.04	-0.04	-0.10	-0.17	A = -0.008		

TABLE 2

VALUES OF C_D AND C_L (C_P)

TRANSONIC SIMILARITY PARAMETER FACTORS

M_∞	0.95	1.00	1.05	1.10	1.15	1.20	1.25		
$\left[\frac{M_\infty^2(\gamma+1)}{\theta^5}\right]^{\frac{1}{3}}$	75.02	77.64	80.23	82.73	85.23	87.68	90.10	10° WEDGE	$\tilde{C}_L = \left[\frac{M_\infty^2(\gamma+1)}{\theta^5}\right]^{\frac{1}{3}} C_L$
	37.97	39.30	40.61	41.88	43.14	44.38	45.60	15° WEDGE	
	23.33	24.15	24.96	25.73	26.51	27.27	28.02	20° WEDGE	
$\frac{\left[M_\infty^2(\gamma+1)\right]^{\frac{1}{3}}}{\theta^{\frac{2}{3}}}$	6.56	6.79	7.02	7.23	7.45	7.67	7.88	10° WEDGE	$\tilde{C}_D = \frac{\left[M_\infty^2(\gamma+1)\right]^{\frac{1}{3}}}{\theta^{\frac{2}{3}}} C_D$
	5.01	5.17	5.35	5.52	5.67	5.85	6.00	15° WEDGE	
	4.11	4.27	4.41	4.53	4.68	4.82	4.94	20° WEDGE	

TABLE 3 (a)

10 THOU. BOTTOM CLEARANCE 20° WEDGE, C_{D_o}, $\tilde{C}_{D_o}$, C_L, $\tilde{C}_L \sim M_\infty$

M_{a_∞}	0.95	1.00	1.05	1.10	1.15	1.20	1.25	INCIDENCE (DEGREES)
$\int_0^1 C_P \, d(\frac{x}{c})$	0.230	0.263	0.299	0.328	0.355	0.380	0.390	0
$\tilde{C}_D$	0.080	0.091	0.104	0.114	0.123	0.132	0.136	
$\tilde{C}_{D_o}$	1.86	2.20	2.60	2.93	3.26	3.60	3.81	
$\int_0^1 C_{P_L} \, d(\frac{x}{c})$	0.257	0.292	0.326	0.358	0.390	0.412	0.430	1
$\int_0^1 C_{P_u} \, d(\frac{x}{c})$	0.198	0.227	0.260	0.290	0.320	0.341	0.353	
C_{D_o}	0.080	0.091	0.103	0.113	0.124	0.132	0.137	
C_L	0.057	0.063	0.063	0.065	0.067	0.068	0.073	
$\tilde{C}_{D_o}$	1.86	2.20	2.57	2.91	3.29	3.60	3.83	
$\tilde{C}_L$	0.23	0.27	0.28	0.29	0.31	0.33	0.36	
$\int_0^1 C_{P_L} \, d(\frac{x}{c})$	0.282	0.320	0.353	0.386	0.416	0.447	0.470	2
$\int_0^1 C_{P_u} \, d(\frac{x}{c})$	0.161	0.193	0.223	0.252	0.277	0.300	0.310	
C_{D_o}	0.081	0.094	0.104	0.115	0.126	0.135	0.141	
C_L	0.117	0.122	0.124	0.128	0.133	0.140	0.153	
$\tilde{C}_{D_o}$	1.88	2.27	2.60	2.96	3.34	3.68	3.95	
$\tilde{C}_L$	0.48	0.52	0.55	0.58	0.62	0.68	0.76	
$\int_0^1 C_{P_L} \, d(\frac{x}{c})$	0.310	0.350	0.386	0.421	0.452	0.488	0.505	3
$\int_0^1 C_{P_u} \, d(\frac{x}{c})$	0.127	0.158	0.187	0.213	0.240	0.260	0.268	
C_{D_o}	0.083	0.096	0.108	0.118	0.128	0.139	0.144	
C_L	0.176	0.189	0.191	0.199	0.202	0.217	0.226	
$\tilde{C}_{D_o}$	1.93	2.32	2.70	3.04	3.39	3.79	4.03	
$\tilde{C}_L$	0.72	0.81	0.84	0.90	0.95	1.05	1.11	

TABLE 3 (a)

10 THOU. BOTTOM CLEARANCE 20° WEDGE, C_{D_0}, $\tilde{C}_{D_0}$, C_L, $\tilde{C}_L$ ~ M_∞

M_{a_∞}	0.95	1.00	1.05	1.10	1.15	1.20	1.25	INCIDENCE (DEGREES)
$\int_0^1 C_{P_L}\, d(\frac{x}{c})$	0.350	0.386	0.425	0.465	0.502	0.537	0.545	4
$\int_0^1 C_{P_u}\, d(\frac{x}{c})$	0.065	0.098	0.128	0.158	0.182	0.205	0.220	
C_{D_0}	0.092	0.104	0.116	0.128	0.140	0.151	0.155	
C_L	0.274	0.277	0.285	0.294	0.306	0.317	0.311	
$\tilde{C}_{D_0}$	2.14	2.51	2.90	3.29	3.71	4.12	4.34	
$\tilde{C}_L$	1.13	1.18	1.26	1.33	1.43	1.53	1.54	
$\int_0^1 C_{P_L}\, d(\frac{x}{c})$	0.396	0.440	0.480	0.507	0.553	0.588	0.590	5
$\int_0^1 C_{P_u}\, d(\frac{x}{c})$	0.020	0.045	0.073	0.100	0.126	0.150	0.172	
C_{D_0}	0.104	0.118	0.130	0.140	0.154	0.165	0.168	
C_L	0.362	0.380	0.390	0.390	0.408	0.416	0.398	
$\tilde{C}_{D_0}$	2.42	2.85	3.25	3.60	4.05	4.50	4.70	
$\tilde{C}_L$	1.48	1.62	1.72	1.76	1.91	2.00	1.96	
$\int_0^1 C_{P_L}\, d(\frac{x}{c})$	0.440	0.483	0.525	0.568	0.610	0.640	0.628	6
$\int_0^1 C_{P_u}\, d(\frac{x}{c})$	-0.028	-0.012	+0.017	0.042	0.070	0.100	0.123	
C_{D_0}	0.119	0.132	0.146	0.159	0.173	0.183	0.182	
C_L	0.450	0.476	0.487	0.503	0.516	0.515	0.480	
$\tilde{C}_{D_0}$	2.78	3.19	3.65	4.10	4.59	5.00	5.10	
$\tilde{C}_L$	1.85	2.03	2.15	2.28	2.42	2.48	2.37	
$\int_0^1 C_{P_L}\, d(\frac{x}{c})$	0.506	0.545	0.584	0.623	0.662	0.690	0.668	7
$\int_0^1 C_{P_u}\, d(\frac{x}{c})$	-0.080	-0.065	-0.037	-0.010	0.015	0.041	0.068	
C_{D_0}	0.144	0.156	0.169	0.181	0.194	0.204	0.199	
C_L	0.564	0.586	0.595	0.605	0.618	0.619	0.571	
$\tilde{C}_{D_0}$	3.36	3.76	4.22	4.66	5.14	5.57	5.57	
$\tilde{C}_L$	2.31	2.50	2.62	2.74	2.89	2.98	2.82	

TABLE 3 (b)

10 THOU. BOTTOM CLEARANCE 15° WEDGE, C_{D_o}, $\tilde{C}_{D_o}$, C_L, $\tilde{C}_L \sim M_\infty$

M_{a_∞}	0.95	1.00	1.05	1.10	1.15	1.20	1.25	INCIDENCE (DEGREES)
$\int_o^1 C_P\, d(\frac{x}{c})$	0.120	0.170	0.210	0.240	0.258	0.268	0.272	0
$\tilde{C}_D$	0.031	0.045	0.055	0.063	0.068	0.070	0.071	
$\tilde{C}_{D_o}$	1.18	1.77	2.23	2.63	2.93	3.11	3.24	
$\int_o^1 C_{P_L}\, d(\frac{x}{c})$	0.198	0.244	0.285	0.317	0.338	0.348	0.342	1
$\int_o^1 C_{P_u}\, d(\frac{x}{c})$	0.077	0.118	0.158	0.195	0.222	0.238	0.243	
C_{D_o}	0.038	0.049	0.060	0.069	0.075	0.079	0.078	
C_L	0.119	0.124	0.125	0.121	0.115	0.108	0.096	
$\tilde{C}_{D_o}$	1.44	1.93	2.43	2.89	3.23	3.50	3.55	
$\tilde{C}_L$	0.59	0.64	0.67	0.67	0.65	0.63	0.58	
$\int_o^1 C_{P_L}\, d(\frac{x}{c})$	0.271	0.320	0.360	0.391	0.411	0.418	0.410	2
$_o C_{P_u}\, d(\frac{x}{c})$	0.034	0.075	0.118	0.155	0.181	0.197	0.203	
C_{D_o}	0.048	0.060	0.070	0.080	0.085	0.088	0.087	
C_L	0.233	0.240	0.238	0.231	0.215	0.216	0.202	
$\tilde{C}_{D_o}$	1.82	2.36	2.84	3.35	3.66	3.90	3.96	
$\tilde{C}_L$	1.16	1.24	1.27	1.27	1.22	1.26	1.21	
$\int_o^1 C_{P_L}\, d(\frac{x}{c})$	0.329	0.384	0.430	0.458	0.470	0.466	0.445	3
$\int_o^1 C_{P_u}\, d(\frac{x}{c})$	-0.006	+0.026	0.065	0.105	0.137	0.154	0.160	
C_{D_o}	0.060	0.072	0.083	0.091	0.097	0.097	0.094	
C_L	0.329	0.351	0.357	0.345	0.325	0.304	0.277	
$\tilde{C}_{D_o}$	2.28	2.73	3.37	3.81	4.18	4.30	4.28	
$\tilde{C}_L$	1.65	1.82	1.91	1.90	1.84	1.78	1.66	
M_{a_∞}	0.95	1.00	1.05	1.10	1.15	1.20	1.25	INCIDENCE (DEGREES)
$\int_o^1 C_{P_L}\, d(\frac{x}{c})$	0.375	0.430	0.475	0.502	0.510	0.500	0.475	4
$\int_o^1 C_{P_u}\, d(\frac{x}{c})$	-0.039	-0.026	0.000	0.033	0.065	0.090	0.100	
C_{D_o}	0.073	0.084	0.095	0.102	0.106	0.105	0.101	
C_L	0.406	0.448	0.465	0.459	0.435	0.400	0.365	
$\tilde{C}_{D_o}$	2.77	3.30	3.85	4.27	4.57	4.66	4.60	
$\tilde{C}_L$	2.03	2.32	2.49	2.53	2.46	2.34	2.19	
$\int_o^1 C_{P_L}\, d(\frac{x}{c})$	0.420	0.470	0.508	0.530	0.532	0.520	0.502	5
$\int_o^1 C_{P_u}\, d(\frac{x}{c})$	-0.085	-0.085	-0.062	-0.031	-0.012	-0.002	-0.002	
C_{D_o}	0.095	0.103	0.110	0.111	0.111	0.110	0.106	
C_L	0.495	0.544	0.557	0.548	0.531	0.509	0.491	
$\tilde{C}_{D_o}$	3.61	4.05	4.46	4.64	4.79	4.88	4.83	
$\tilde{C}_L$	2.48	2.81	2.98	3.02	3.01	2.97	2.94	

TABLE 4 (a)

$\tilde{C}_{D_o}$ and $\tilde{C}_L \sim M_\infty,\ \alpha(\xi_\infty,\ \tilde{\alpha})$ 15° WEDGE

$\tilde{C}_{D_o}$	α°	0.75	1.50	2.25	3.00	3.75	4.5	
M_∞								ξ_∞
0.95		1.37	1.62	1.93	2.29	2.72	3.20	-0.23
1.00		1.87	2.08	2.38	2.74	3.17	3.65	0.00
1.05		2.37	2.62	2.97	3.36	3.74	4.13	0.21
1.10		2.80	3.10	3.47	3.84	4.17	4.46	0.40
1.15		3.13	3.43	3.80	4.19	4.49	4.69	0.58
1.20		3.39	3.70	4.01	4.30	4.57	4.77	0.74
1.25		3.47	3.75	4.04	4.30	4.53	4.72	0.90
$\tilde{C}_L$	α°	0.75	1.50	2.25	3.00	3.75	4.5	
M_∞								ξ_∞
0.95		0.44	0.87	1.27	1.65	2.00	2.30	-0.23
1.00		0.48	0.93	1.38	1.81	2.22	2.58	0.00
1.05		0.49	0.97	1.45	1.91	2.34	2.73	0.21
1.10		0.49	0.97	1.45	1.92	2.37	2.79	0.40
1.15		0.46	0.92	1.37	1.84	2.29	2.73	0.58
1.20		0.44	0.88	1.32	1.76	2.21	2.65	0.74
1.25		0.40	0.81	1.22	1.63	2.05	2.52	0.90
$\frac{t}{o\alpha}$		10.00	5.00	3.33	2.50	2.00	1.67	
$\tilde{\alpha}$		0.1	0.2	0.3	0.4	0.5	0.6	

TABLE 4 (b)

$\tilde{C}_{D_o}$ and $\tilde{C}_L \sim M_\infty,\ \alpha(\xi_\infty,\ \tilde{\alpha})$ 20° WEDGE

$\tilde{C}_{D_o}$	α°	1.00	2.00	3.00	4.00	5.00	6.00	7.00	
M_∞									ξ_∞
0.95		1.86	1.88	1.93	2.14	2.42	2.78	3.36	-0.18
1.00		2.20	2.27	2.32	2.51	2.85	3.19	3.76	0.00
1.05		2.57	2.60	2.70	2.90	3.25	3.65	4.22	0.17
1.10		2.91	2.96	3.04	3.29	3.60	4.10	4.66	0.33
1.15		3.29	3.34	3.39	3.71	4.05	4.59	5.14	0.48
1.20		3.60	3.68	3.79	4.12	4.50	5.00	5.57	0.61
1.25		3.83	3.95	4.03	4.34	4.70	5.10	5.57	0.74
$\tilde{C}_L$	α°	1.00	2.00	3.00	4.00	5.00	6.00	7.00	
M_∞									ξ_∞
0.95		0.23	0.48	0.72	1.13	1.48	1.85	2.31	-0.18
1.00		0.27	0.52	0.81	1.18	1.62	2.03	2.50	0.00
1.05		0.28	0.55	0.84	1.26	1.72	2.15	2.62	0.17
1.10		0.29	0.58	0.90	1.33	1.76	2.28	2.74	0.33
1.15		0.31	0.62	0.95	1.43	1.91	2.42	2.89	0.48
1.20		0.33	0.68	1.05	1.53	2.00	2.48	2.98	0.61
1.25		0.36	0.76	1.11	1.54	1.96	2.37	2.82	0.74
$\frac{t}{o}$		10.00	5.00	3.33	2.50	2.00	1.67	1.43	
		0.1	0.2	0.3	0.4	0.5	0.6	0.7	

TABLE 5

$\tilde{C}_{P_{u(L)}}$ FOR ZERO INCIDENCE ~ ξ_∞

% c	5	10	20	30	40	50	60	70	80	90	95	M_∞	ξ_∞	WEDGE
	2.10	1.85	1.30	1.30	0.90	0.54	0.00	0.00	0.00	-0.93	-1.50	0.95	-0.22	15°
	3.32	2.24	1.87	1.87	1.25	1.15	1.15	0.87	0.87	0.18	-0.97	1.01	0.04	15°
	3.03	2.59	1.59	1.40	1.11	1.02	0.34	0.34	0.00	-0.43	-0.82	1.06	0.24	15°
	2.95	2.69	2.30	1.94	1.78	1.44	1.13	1.13	1.05	0.19	0.45	1.14	0.56	15°
	3.79	2.61	1.99	1.80	1.73	1.31	1.23	1.15	1.01	0.66	0.49	1.20	0.74	15°
	2.34	1.79	1.51	1.24	1.16	0.69	0.42	0.42	0.24	-0.17	-1.08	1.00	0.00	15°

TABLE 6

ERRORS IN RESULTS DUE TO INITIAL READING ERROR OF 0.02"

NUMBER OF RUN	1	2	3	4	5	6
M_{w_∞}	0.94	0.94	0.94	1.29	1.29	1.29
M_{a_∞}	0.95	0.95	0.95	1.25	1.25	1.25
h'	3.20	3.42	3.52	2.94	3.20	3.40
d	0.316	0.249	0.218	0.395	0.316	0.255
d/d_∞	1.264	1.000	0.872	1.580	1.264	1.020
M_w	0.525	0.940	0.988	0.568	0.950	1.265
M_a	0.550	0.950	0.990	0.590	0.960	1.23
C_P	0.72	0.00	-0.07	+0.96	0.395	0.025
$h' + \Delta h'$	3.18	3.40	5.50	2.92	3.18	3.38
$\alpha + \Delta d$	0.322	0.255	0.224	0.401	0.322	0.461
$\frac{\alpha + \Delta d}{d_\infty - \Delta d_\infty}$	1.325	1.050	0.922	1.650	1.325	1.075
$M_w + \Delta M_w$	0.400	0.868	1.065	0.460	0.885	1.188
$M_a + \Delta M_a$	0.425	0.880	1.060	0.490	0.900	1.160
$C_P + \Delta C_P$	0.930	0.125	-0.185	1.100	0.485	0.115
ΔC_P	0.210	0.125	0.115	0.140	0.090	0.090

CASE	ΔC_{D_o}	$C_{D_{o_{MIN}}}$	POSSIBLE % ERROR
20° WEDGE 7° INCIDENCE	0.034	0.144	24
10° WEDGE 6° INCIDENCE	0.017	0.016	100

CASE	C_L	$C_{L_{MIN}}$	POSSIBLE % ERROR
20° WEDGE 7° INCIDENCE	0.196	0.564	35
10° WEDGE 1° INCIDENCE	0.200	0.109	184

Assume an error in C_P of 0.10 whence $\int_0^1 \Delta C_P \, d(\frac{x}{c}) = 0.1$.

We then have the following cases, shown on the right hand side.

$h' = 3.42$ $\qquad d_\infty = 0.249$

$h' + \Delta h' = 3.44$ $\qquad d_\infty - \Delta d_\infty = 0.243$

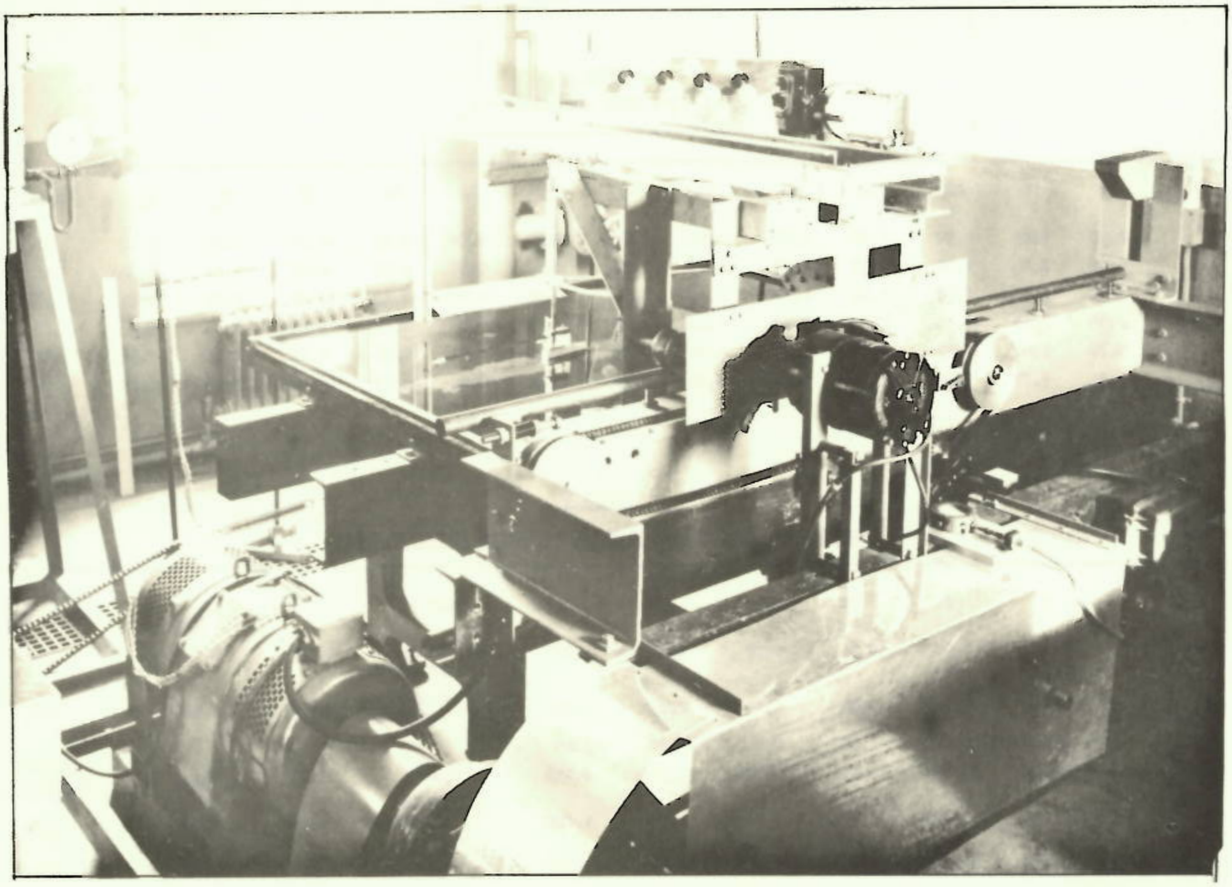

FIG. 1. GENERAL VIEW OF APPARATUS SHOWING DRIVE MECHANISM

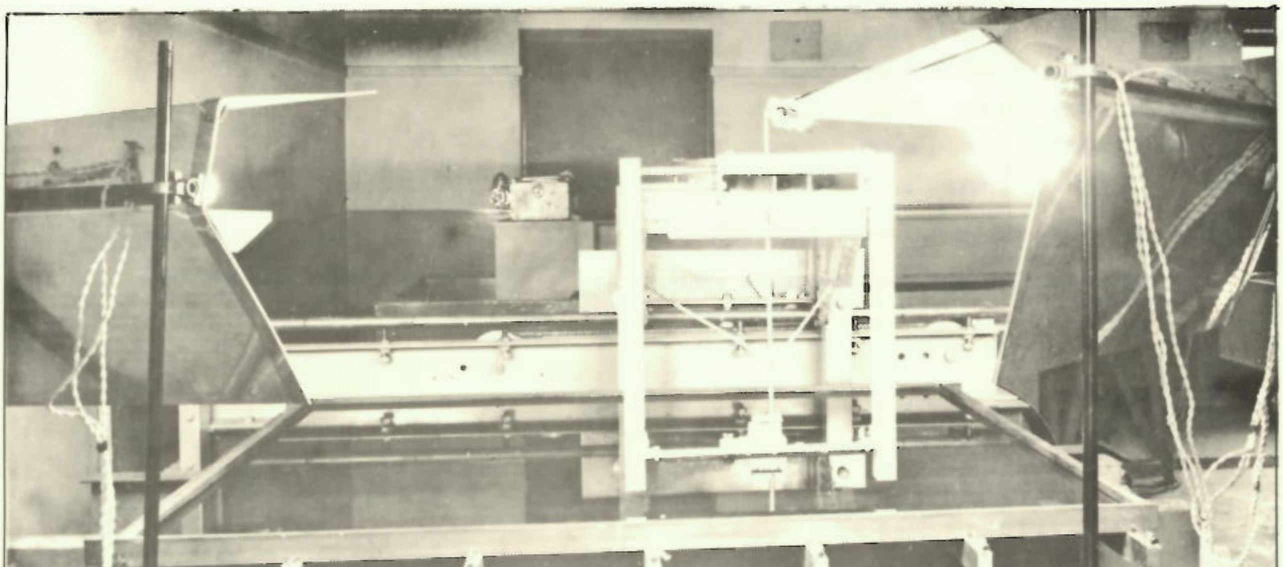

FIG. 2. GENERAL VIEW OF APPARATUS SHOWING MODEL MOUNTING AND CAMERA PLATFORM

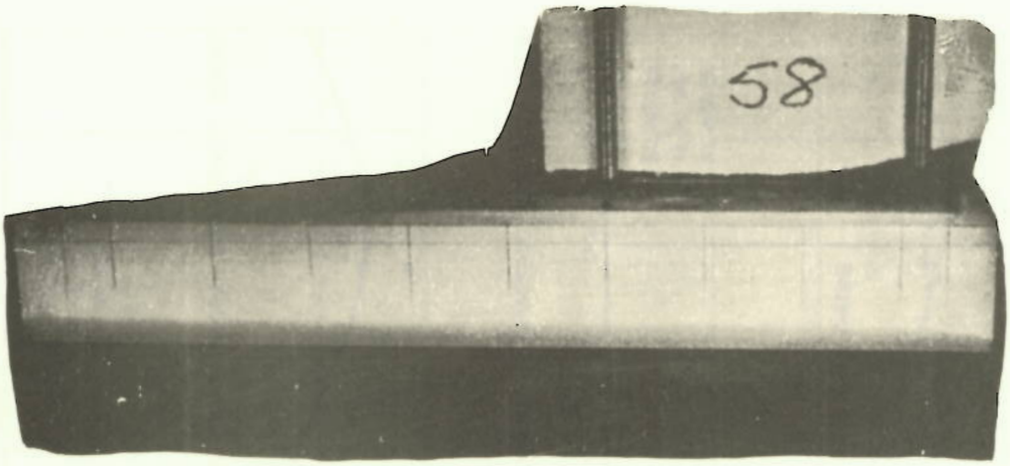

FIG. 3. 15° WEDGE $\alpha = 0^{\circ}$, CLEARANCE 0.010", $M_{\infty} = 0.98$

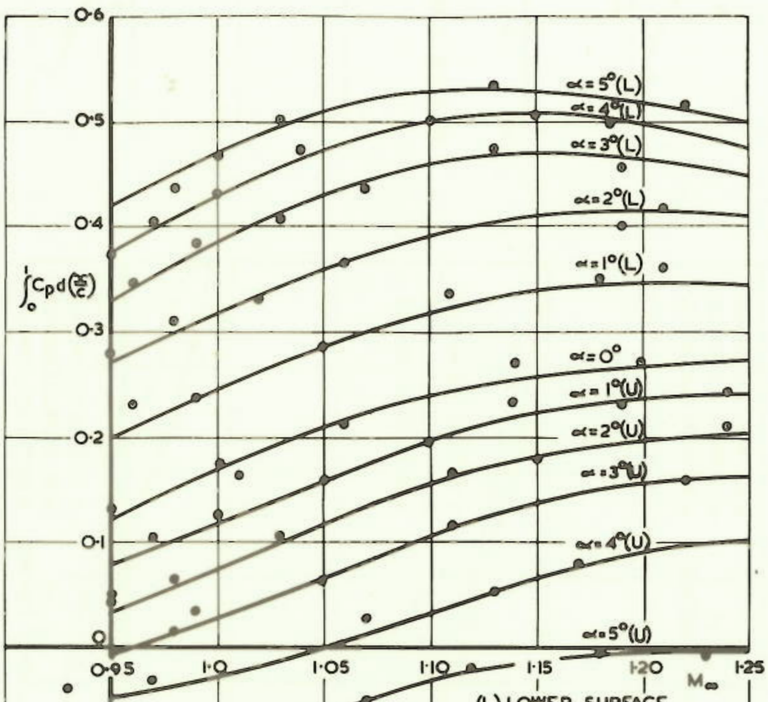

FIG. 4. VARIATION OF THE INTEGRATED PRESSURE DISTRIBUTION WITH FREESTREAM MACH NUMBER. 15° WEDGE

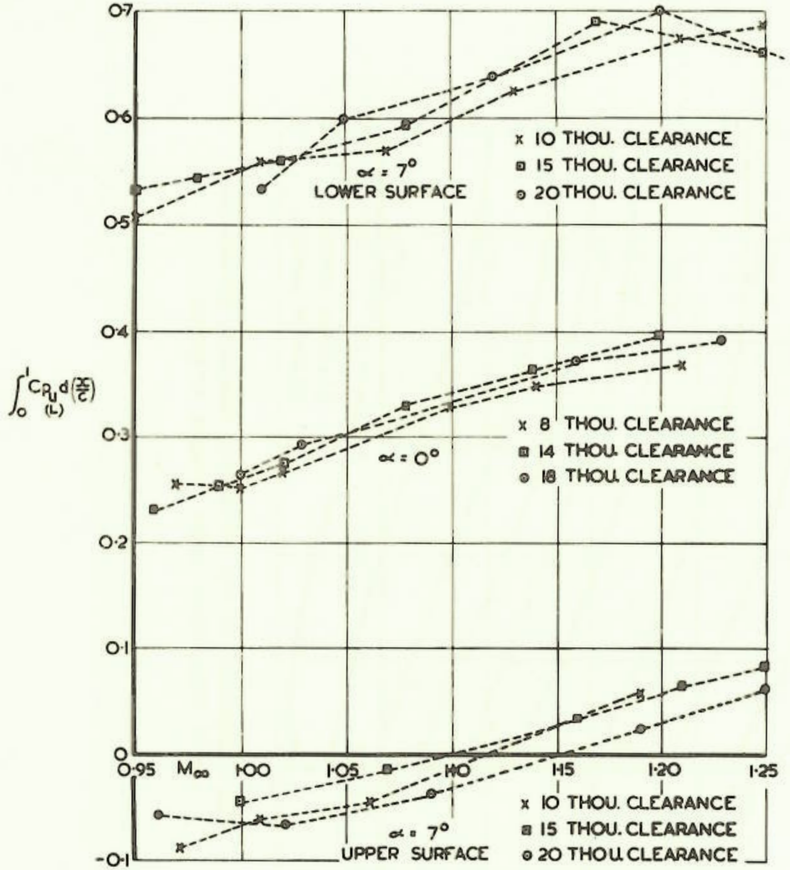

FIG.5. THE EFFECT OF BOTTOM CLEARANCE. 20° WEDGE

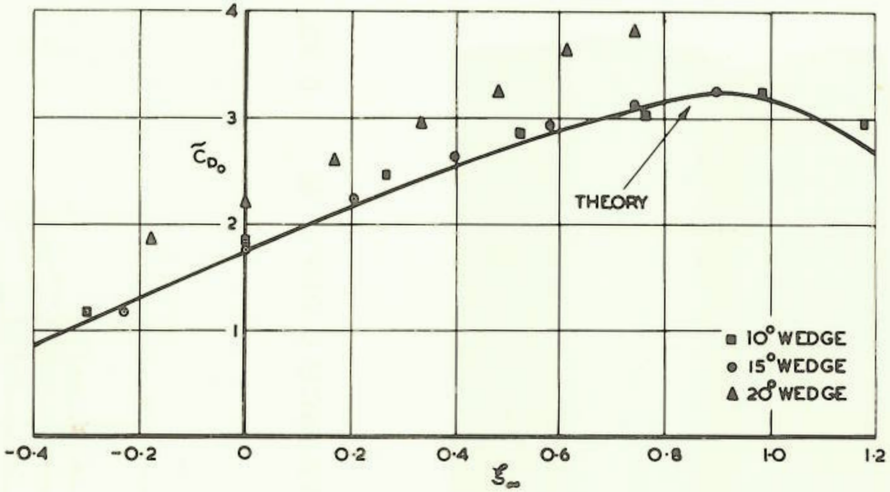

FIG.6. THE ZERO INCIDENCE DRAG COEFFICIENTS IN TRANSONIC SIMILARITY FORM

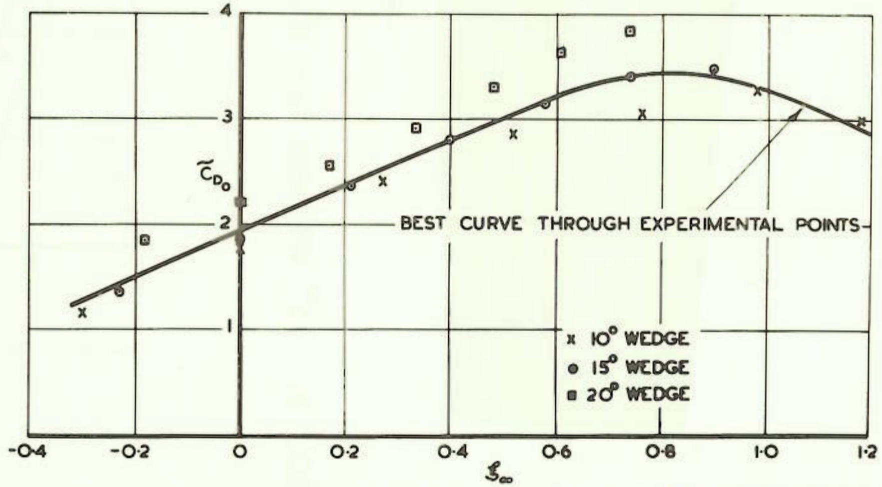

FIG.7. GENERALISED DRAG COEFFICIENT VERSUS TRANSONIC SIMILARITY PARAMETER FOR $\tilde{\alpha} = 0·1$

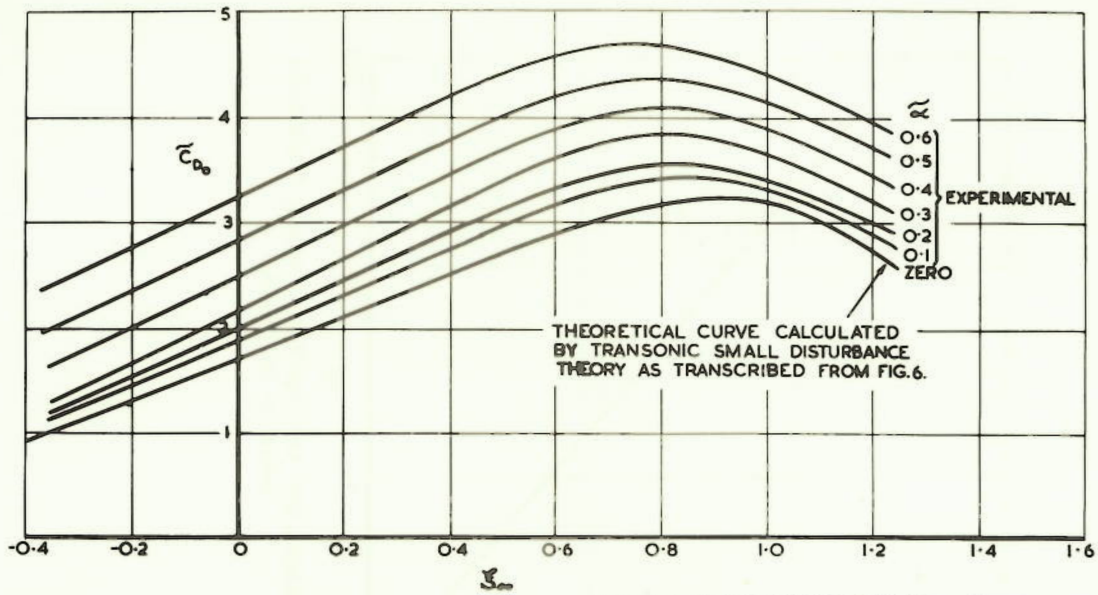

FIG. 8. THE DRAG COEFFICIENTS OF SINGLE WEDGE SECTIONS IN TRANSONIC SIMILARITY FORM

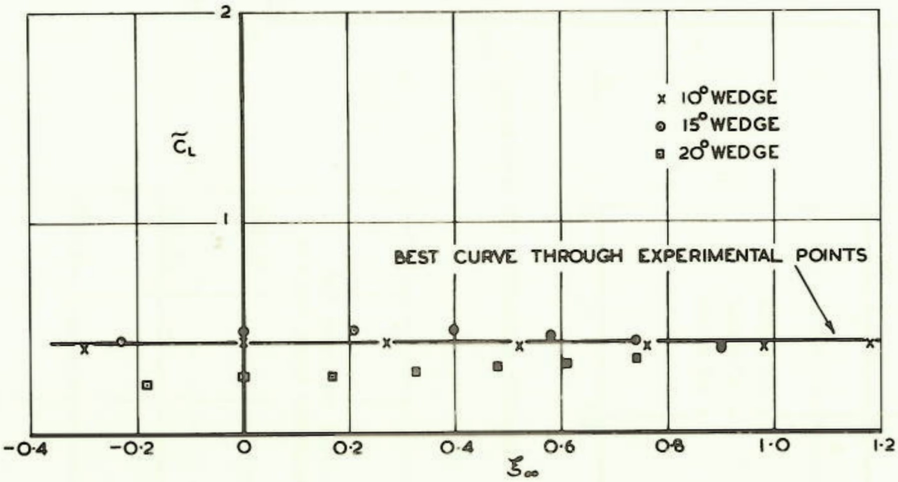

FIG. 9. GENERALISED LIFT COEFFICIENT VERSUS TRANSONIC SIMILARITY PARAMETER FOR $\tilde{\alpha} = 0{\cdot}1$

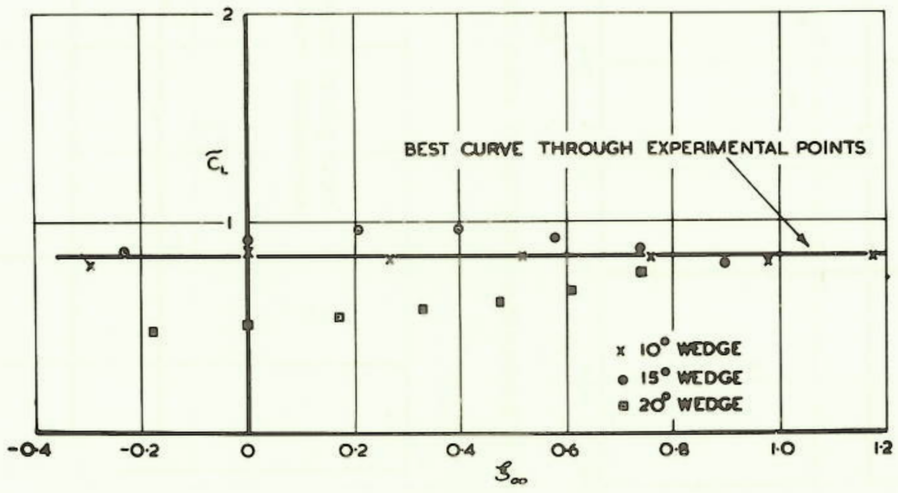

FIG. 10. GENERALIZED LIFT COEFFICIENT VERSUS TRANSONIC SIMILARITY PARAMETER FOR $\tilde{\alpha} = 0{\cdot}2$

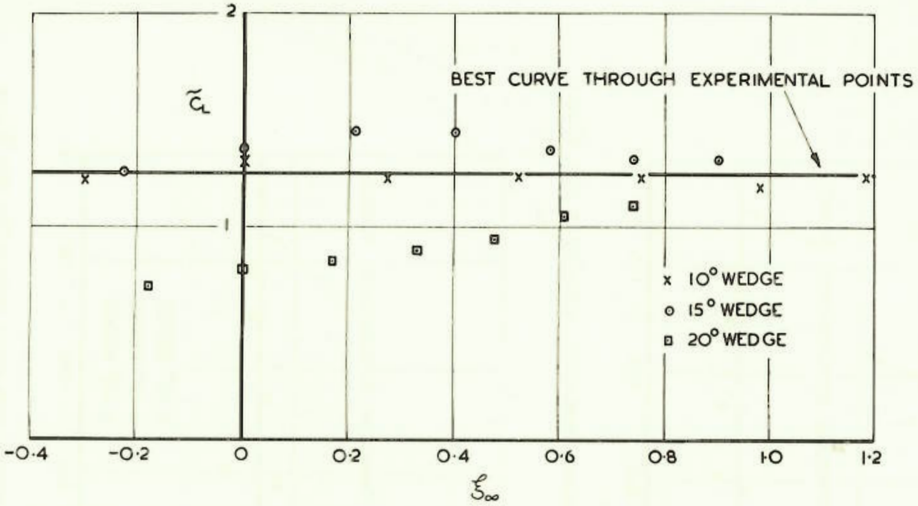

FIG. 11. GENERALIZED LIFT COEFFICIENT VERSUS TRANSONIC SIMILARITY PARAMETER FOR $\tilde{\alpha} = 0·3$

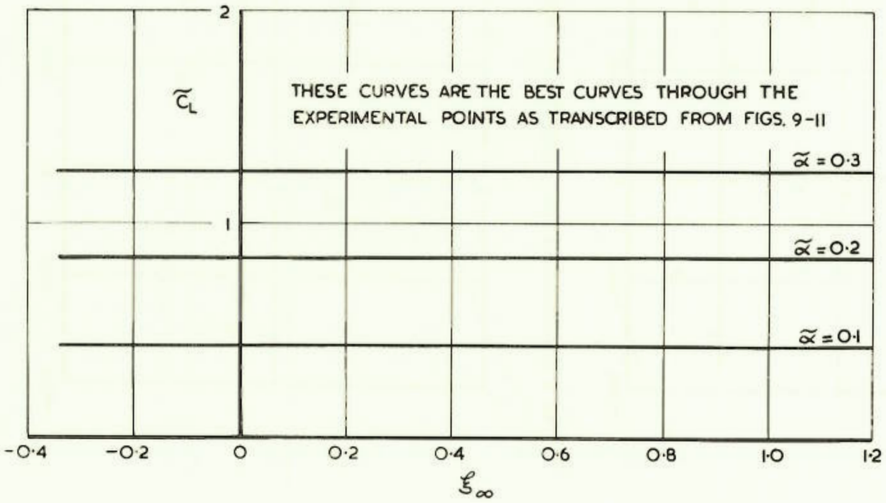

FIG. 12. THE LIFT COEFFICIENTS OF SINGLE WEDGE SECTIONS IN TRANSONIC SIMILARITY FORM

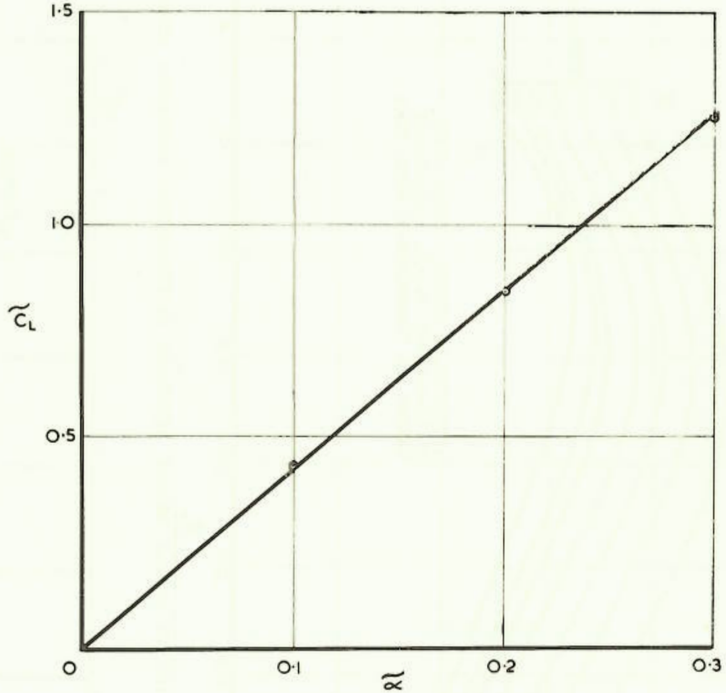

FIG 12a GENERALIZED LIFT COEFFICIENT VERSUS GENERALIZED ANGLE OF INCIDENCE

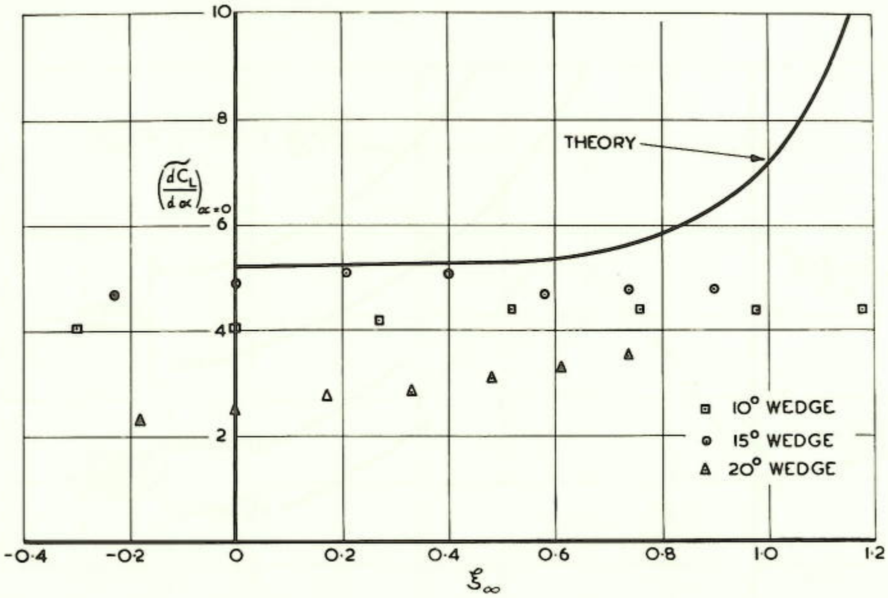

FIG. 13. THE LIFT CURVE SLOPE AT ZERO INCIDENCE IN TRANSONIC SIMILARITY FORM

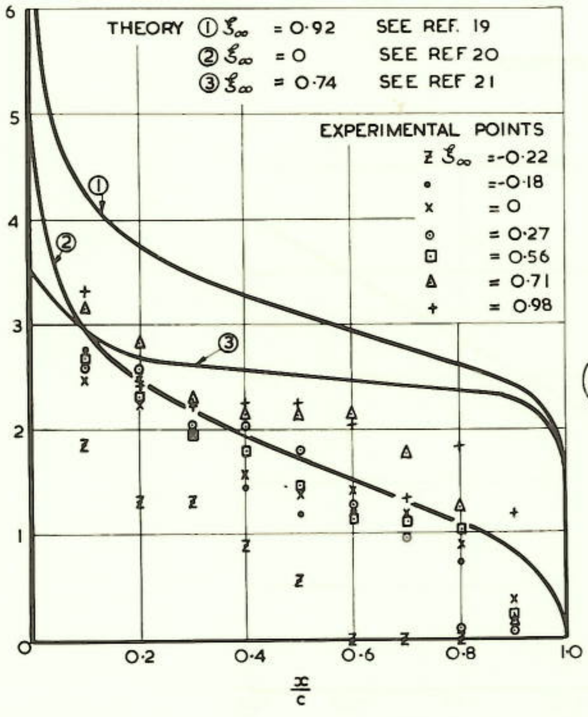

FIG. 14. THE ZERO INCIDENCE CHORDWISE GENERALISED PRESSURE COEFFICIENT DISTRIBUTION

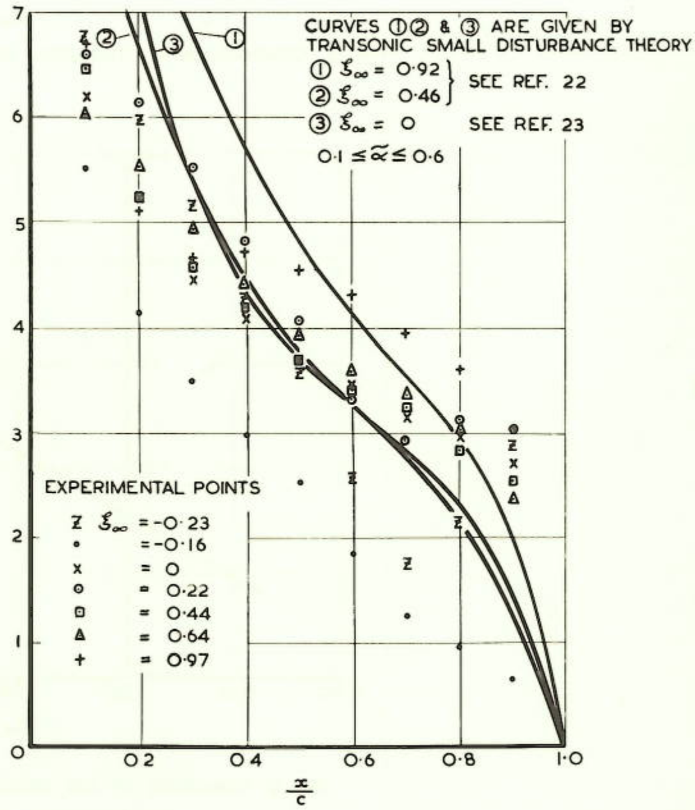

FIG. 15. CHORDWISE LIFT DISTRIBUTION IN TRANSONIC SIMILARITY FORM

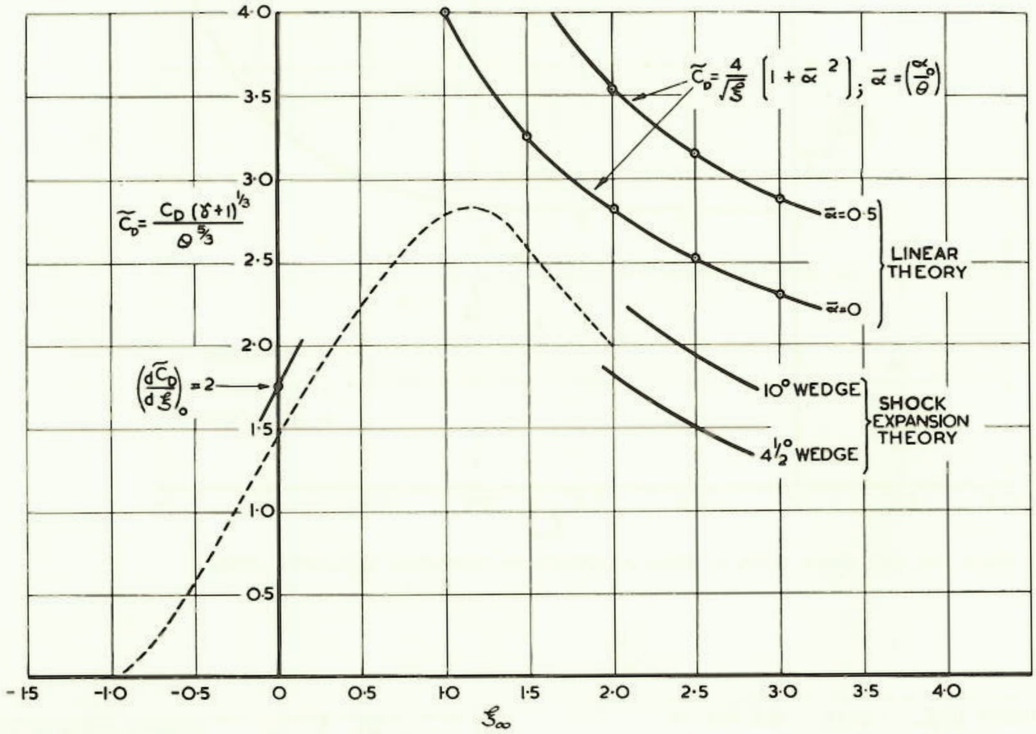

FIG. 16. COMPARISON OF THEORIES WITH EXPERIMENT

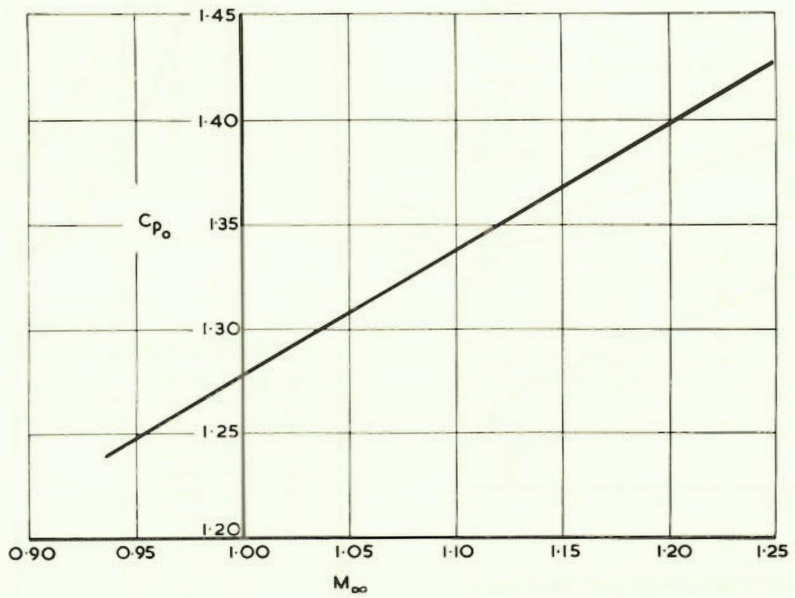

FIG. 17. VARIATION OF THE STAGNATION PRESSURE COEFFICIENT WITH FREESTREAM MACH NUMBER

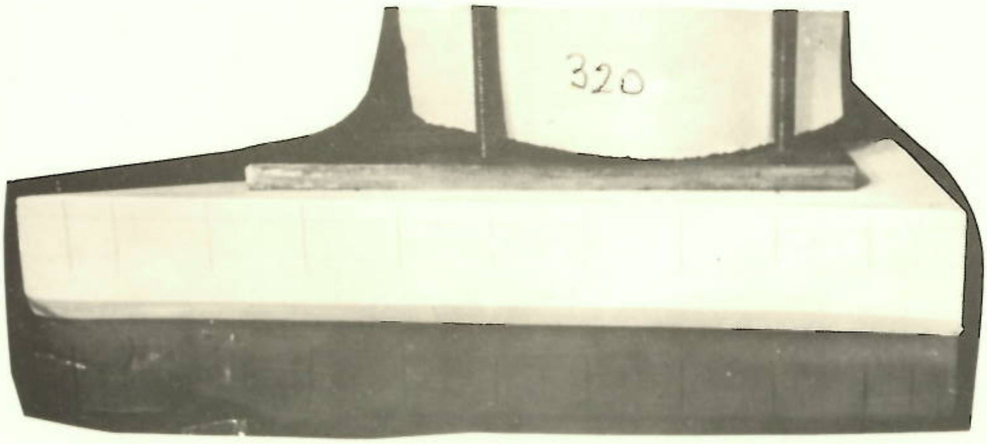

FIG. 18. 20° WEDGE, α = 5°, UPPER SURFACE, CLEARANCE 0.010", M_∞ = 1.09

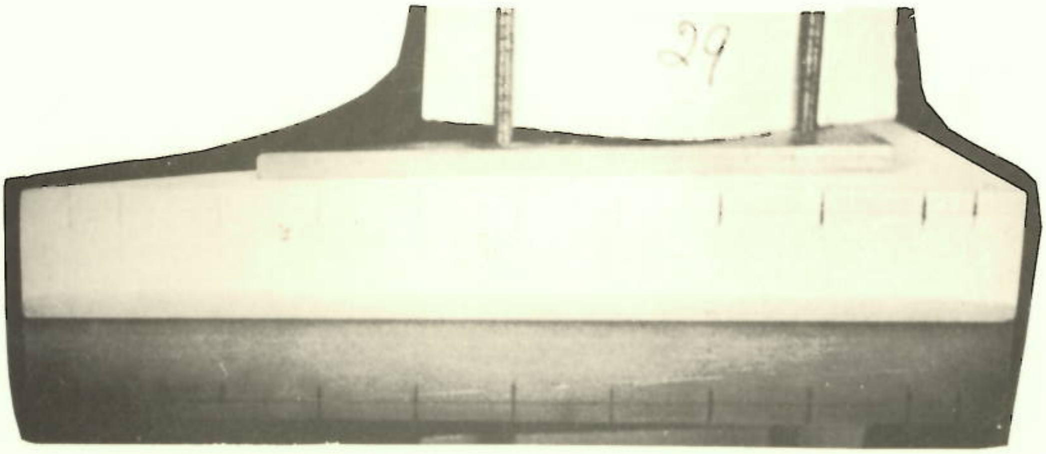

FIG. 19. 20° WEDGE, α = 0°, CLEARANCE 0.018", STILL

FIG. 20. 20° WEDGE, α = 3°, UPPER SURFACE, CLEARANCE 0.010", M_∞ = 1.28